Hydraulics Research
Wallingford

A TWO-DIMENSIONAL MODEL OF THE MOVEMENT OF FLUID MUD IN A HIGH ENERGY TURBID ESTUARY

Nicholas V M Odd BSc FICE

Alan J Cooper MA PhD

Report No SR 147
January 1988

Registered Office: Hydraulics Research Limited,
Wallingford, Oxfordshire OX10 8BA.
Telephone: 0491 35381. Telex: 848552

This report describes work funded by the Department of the Environment under Research Contract PECD 7/6/58 for which the DoE nominated officer was Dr R P Thorogood. It is published on behalf of the Department of the Environment, but any opinions expressed in this report are not necessarily those of the funding Department. The work was carried out by Mr N V M Odd and Dr A J Cooper in the Tidal Engineering Department of Hydraulics Research, Wallingford, under the management of Mr M F C Thorn.

ABSTRACT

Fluid mud is a dense suspension containing a concentration of mud flocs which is high enough to change significantly the physical properties of the mud/water mixture compared to that of clear water at the same salinity and temperature. Fluid mud is formed under a variety of conditions. Once formed it may flow under the influence of gravity and hydrostatic forces and then settle and dewater in navigation channels and berths, causing siltation over and above that due to settlement directly from suspension. The movement of fluid mud has been cited as the most likely cause of rapid siltation in the majority of the ports in the world located in muddy estuaries. In the past, it has been very difficult to predict or quantify this extra siltation, which may in some cases double the annual maintenance dredging bill for a new port extension.

Fluid mud is defined as being a flocculated suspension of mud particles in the range 60,000 to 120,000ppm, but more typically with a value of about 75,000ppm. For engineering calculations one can probably assume that it has a yield shear strength of about 0.1 N/m^2 and a viscosity about twice that of water.

A general theory in the form of partial differential equations and empirical relationships was devised to described the formation, motion and dewatering of a fluid mud layer in two dimensions in plan. The theory was incorporated as a subroutine and run interactively with HR's standard two-dimensional depth-averaged tidal flow and suspended mud transport models (TIDEFLOW-2D and MUDFLOW-2D).

The new model simulated the interchange of mud between the suspended mud, fluid mud and settled mud phases. Once formed, the relatively thin fluid mud layer was assumed to move under the action of gravitational, hydrostatic and frictional forces, without feed-back on the motion of the overlying water.

The new modelling method was used to set up a pilot model of mud transport in the Severn Estuary. The mud transport model was driven using results from the two-dimensional tidal flow model developed for the Bondi study. Simplified initial and boundary conditions for suspended mud concentrations were based on observations.

The main purpose of the exercise was to attempt to simulate the main features of the spatial and temporal patterns of the formation of fluid mud observed with an echo-sounder by Kirby and Parker, which are reviewed in the report. The model showed that it is possible to simulate the main processes causing the growth, motion and re-entrainment of ephemeral fluid mud layers in a high energy turbid estuary such as the Severn Estuary.

The main processes are:

Settlement of suspended mud into the lower layers of the flow as the vertical turbulent flux decreases near slack water.

A negligible or very slow rate of dewatering of the fluid mud.

Flow by gravity down the sloping bed into deep channels.

Flow along deep channels under the action of hydrostatic forces generated by the slope of the water surface.

Entrainment by the overlying flow.

The main findings as regards the simulation of conditions in the Severn Estuary are:

The importance of the lateral flow of fluid mud from the side slopes concentrating the mud in the deep channels located mainly on the English side of the estuary.

The manner in which fluid mud is rapidly re-suspended by entrainment by the overlying water after slack water, thereby greatly increasing the mobility of the sediments.

The contribution that the mass movement of mud in the fluid mud layer makes to the total mud transport in the estuary.

The main weaknesses of the modelling techniques are:

The lack of resolution of the suspended mud concentration profile in a 2-dimensional depth-averaged mud transport model.

The lack of firm field evidence that fluid mud behaves as a Bingham fluid with a lower yield strength. The present value of $0.1N/m^2$ is based on rotating viscometer measurements made in 1962.

The lack of evidence for defining the rate of dewatering of fluid mud, which is at present based on a single laboratory measurement made with clay in fresh water.

The lack of evidence that the fluid mud is entrained in a similar manner to salt in a stationary saline wedge.

The lack of field observations which are capable of separating mobile fluid mud with density of about 1.07 Tonnes/m^3 and a stationary low density soil with salinity of about 1.2 Tonnes/m^3.

The proposed modelling method cannot be used to make firm predictions of the effects of engineering works on mud transport in turbid high energy estuaries until there is more solid evidence and justification for some of the basic assumptions and the values of the coefficients described in this report.

At its present stage of development the modelling method can only be applied to make a preliminary assessment of the importance of fluid mud in maintaining the pattern of mud transport and siltation in a particular estuary.

CONTENTS

FIGURES

1 INTRODUCTION

Fluid mud is a dense suspension containing a concentration of mud flocs which is high enough to significantly change the physical properties of the mud/water mixture compared to that of clear water with the same salinity and temperature.

Fluid mud is formed under a variety of conditions. Once formed it may flow under the influence of gravity and hydrostatic forces and then settle and dewater in navigation channels and berths, causing significant rates of siltation over and above that due to settlement directly from suspension.

This report describes how the theories developed by Odd and Rodger in HR Report SR 84 (March 1986) (Ref 1) were incorporated into an existing standard HR two-dimensional computational mud transport model, MUDFLOW-2D.

Fluid mud is a common phenomenon in the Severn Estuary. So it was decided to use tidal flow results from the 500 metre gridded model developed for the Bondi Study (Ref 2) to drive a pilot model of mud transport in the Severn Estuary.

It should be appreciated that the pattern of mud transport in the Severn Estuary is too complicated to be simulated accurately in a pilot model. However, the main purpose of the exercise was to demonstrate the ability of the model to simulate the various features of the motion and behaviour of deep fluid mud layers in a high energy estuary.

The theoretical basis and assumptions of the two dimensional model of the formation, movement and dewatering of a fluid mud layer are set out in Chapter 2.

Dr Alan Cooper programmed the numerical solution of the partial differential equations in DAP Fortran for implementation on the HR 64 x 64 DAP computer, which is described in Chapter 3. The observations of fluid mud layers in the Severn Estuary are discussed in Chapter 4. The simulation of conditions in the Severn Estuary is described in Chapter 5.

2 THEORY FOR MOVEMENT OF FLUID MUD IN TWO DIMENSIONS

The fluid mud is considered to be a Bingham fluid with a uniform density $(\rho_o + \Delta\rho)$. The partial differential equations which govern the conservation of volume, mass and momentum of the fluid mud layer are as follows:-

<u>Conservation of volume and mass of mud</u>

$$\frac{\partial d_m}{\partial t} + \frac{\partial u_m d_m}{\partial x} + \frac{\partial v_m d_m}{\partial y} - \frac{1}{C_o}\frac{dm}{dt} = 0 \qquad (1)$$

Where

d_m is the thickness of the fluid mud layer (m)

u_m and v_m are the depth averaged velocity components referred to Cartesian co-ordinates x and y (m/s).

$\frac{dm}{dt}$ is the net rate of mass exchange of mud ($kg/m^2/s$)

C_o is the constant concentration of the mud in the fluid mud layer ($75kg/m^3$). The net rate of mass exchange of mud, $\frac{dm}{dt}$, between the fluid mud layer, the water column above and the solid mud bed below is the result of four processes.

Settlement of mud flocs from suspension in the overlying water column. This occurs when the rate of vertical turbulent exchange at the upper interface is insufficient to keep the mud flocs in suspension. For the purposes of the model this was defined in terms of a critical bed stress τd_m below which settlement from suspension was assumed to occur. The value of τd_m is expected to be considerably higher than the critical value for deposition on to the bed ($\tau_d = 0.1\ N/m^2$).

The vertical flux of mud settling into the fluid mud layer is,

$$\frac{dm}{dt} = V_s(C)\ C\ H\left[\tau d_m - \tau_o\right](1 - \frac{\tau o}{\tau d_m})\ (kg/m^2/s) \qquad (2)$$

Where

V_s (C) is the settling velocity (m/s) of the mud at concentration C

C is the concentration of suspended mud in the over lying water column (kg/m^3)

τ_o is the shear stress at the water/bed interface. (N/m^2)

τd_m is the critical stress below which settlement can occur (N/m^2)

H [x] is a Heavyside function such that

H [x] = 1 when x is positive

H [x] = 0 when x is negative

The overlying water will entrain mud from the fluid mud layer if the bulk Richardson Number, Ri_B, is less than 10.

Where

$$Ri_B = \frac{\Delta\rho\ g\ d_m}{(\Delta U)^2} \qquad (3)$$

And

$$\Delta\rho = 0.62\ C_o \qquad Kg/m^3 \qquad (4)$$

g is the gravitation constant (9.81 m/s/s)

ΔU is the velocity difference between the overlying water and the fluid mud.

The vertical flux of mud entrained from the mud layer is assumed to be similar to that for salt in a saline wedge (Ref 3):

$$\frac{dm}{dt} = - V_e\ C_o\ H\ [Ri_B - 10] \qquad (Kg/m^2/s) \qquad (5)$$

$$V_e = \Delta U \frac{0.1}{(1 + 63Ri_B{}^2)^{3/4}}$$

Where

V_e is the entrainment velocity

$$\Delta U = (\Delta u^2 + \Delta v^2)^{1/2} \qquad (6)$$

Where

$\Delta u = u - u_m$

$\Delta v = v - v_m$

Where u and v (m/s) are the depth averaged horizontal velocity (m/s) components in the overlying water. Normally, one would not expect entrainment of mud from the fluid mud layer to occur at the same time as settlement from suspension.

When a fluid mud layer is at rest ($u_m = 0$, $v_m = 0$) it is assumed to dewater at a constant rate.

$$\frac{dm}{dt} = V_o\ C_o \qquad (Kg/m^2/s) \qquad (7)$$

if $u_m = o$ and $v_m = o$.

Where

$V_o = 5 \times 10^{-5}$ m/s

$C_o = 75$ kg/m^3

If the fluid mud is moving rapidly across a muddy bed it may erode it. This is likely to occur if τ_m exceeds τ_e.

In this case the increase in mass of mud in the fluid mud layer is:

$$\frac{dm}{dt} = H\left[\tau_m - \tau_e\right] m_e \left(\tau_m - \tau_e\right) \quad (Kg/m^2/s) \qquad (8)$$

Where

τ_m is the shear stress between the fluid mud and the underlying mud bed. (N/m^2)

τ_e is the critical shear stress for erosion of the bed surface deposits. (N/m^2)

m_e is an erosion constant (Kg/N/s)

In the absence of a fluid mud layer the exchanges between the suspended mud in the overlying water and the bed are assumed to occur as follows:

Definition for deposition onto the bed

If

$$C_o V_o > V_s (C) C$$

So

$$\frac{dm}{dt} = V_s (C) \qquad C \left(1 - \frac{\tau_d}{\tau}\right) \quad (Kg/m^2/s) \qquad (9)$$

Where

τ is the bed shear stress assuming a smooth mud bed ($f = 0.008$).

Erosion into suspension. If $\tau \geq \tau_e$

then

$$\frac{dm}{dt} = m_e \, (\tau - \tau_e) \quad (Kg/m^2/s) \qquad (10)$$

<u>Conservation of momentum in the fluid mud layer</u>

The overlying water is assumed to a have a uniform density ρ_o and the fluid mud to have a uniform density $\rho_o + \Delta\rho$. The equation of motion in the x direction is:-

$$\frac{\partial u_m}{\partial t} + u_m \frac{\partial u_m}{\partial x} + v_m \frac{\partial u_m}{\partial y} + \frac{g\partial \eta}{\partial x} + \frac{g\Delta\rho}{(\rho_o + \Delta\rho)} \left(\frac{\partial \eta_m}{\partial x} - \frac{\partial \eta}{\partial x}\right)$$

$$- D\left(\frac{\partial^2 u_m}{\partial x^2} + \frac{\partial^2 u_m}{\partial y^2}\right) - \Omega v + \frac{1}{d_m(\rho_o + \Delta\rho)} \{\tau_o + \tau_B - \tau_i\} = 0 \quad (11)$$

The convective acceleration and eddy diffusion terms are assumed to be small compared to the other terms.

$$\frac{\partial u_m}{\partial t} + g \frac{\partial \eta}{\partial x} + \frac{g\Delta\rho}{(\rho_o + \Delta\rho)} \left(\frac{\partial \eta_m}{\partial x} - \frac{\partial \eta}{\partial x} \right) - \Omega v$$

$$+ \frac{1}{d_m (\rho_o + \Delta\rho)} \left\{\tau_o + \tau_B \frac{u_m}{(u_m^2 + v_m^2)^{\frac{1}{2}}} - \tau_i\right\} = o \qquad (12)$$

Similarly the equation of motion in the y direction is

$$\frac{\partial v_m}{\partial t} + g \frac{\partial \eta}{\partial y} + \frac{g\Delta\rho}{(\rho_o + \Delta\rho} \left(\frac{\partial \eta_m}{\partial y} - \frac{\partial \eta}{\partial y}\right) - \zeta u$$

$$+ \frac{1}{d_m} \left(\rho_o + \Delta\rho\right) \left\{\tau_o + \tau_B \frac{V_m}{u_m^2 + V_m^2} - \tau_i\right\} \cdot = o \qquad (13)$$

$$\tau_o = \frac{f\rho_m}{8} u_m \left(u_m^2 + v_m^2\right)^{1/2} \qquad (14)$$

$$\tau_i = \frac{f\rho_m}{8} \Delta u \left(\Delta u^2 + \Delta v^2\right)^{1/2} \qquad (15)$$

$$\Delta u = u - u_m$$

$$\Delta v = v - v_m$$

Where

f is the friction factor (≈ 0.008)

η is the water surface level relative to a common datum (m)

$\eta_m = \eta_o + d_m$ is the interface level relative to a common datum (m)

η_o is the bed surface level relative to a common datum (m)

Ω is the Coriolis parameter (s^{-1})

τ_B is the Bingham yield stress strength of the fluid mud (≈ 0.1 N/m^2)

τ_o is the bed shear stress (N/m^2)

τ_i is the interface shear stress (N/m^2)

$\rho_m = \rho_o + \Delta\rho$ is the density of the mud/water mixture (Kg/m^3)

3 NUMERICAL METHOD USED TO SOLVE THE FLUID MUD FLOW EQUATIONS

The fluid mud flow equations were added to the existing MUDFLOW-2D program. This program uses the parallel processing facility of the ICL DAP at HR. The numerical model grid has the suspended mud concentration (c) computed at the centre of the cell and the u velocity and the v velocity on the east and south faces respectively. The model uses explicit upstream differences so the flux F_x of suspended mud in the x direction is given by:

$$F^{n+\frac{1}{2}}_{xij} = u^{n+\frac{1}{2}}_{ij} \Delta t \, \Delta y \, c^{n}_{ij} d \quad (u^{n+\frac{1}{2}}_{ij} > 0)$$

$$= u^{n+\frac{1}{2}}_{ij} \Delta t \, \Delta y \, c^{n}_{i+1j} d \quad (u^{n+\frac{1}{2}}_{ij} < 0)$$

ie the flux is computed from the concentration in the donor cell. In this notation the superscript denotes timestep number and the subscripts are row and column counters and d is the water depth. Given the fluxes the new concentration is given by:

$$c^{n+1}_{ij} = c^{n}_{ij} + (F^{n+\frac{1}{2}}_{xi-1j} + F^{n+\frac{1}{2}}_{yij} - F^{n+\frac{1}{2}}_{yij-1} - F^{n+\frac{1}{2}}_{xij}) / \Delta x \, \Delta y d + \text{source terms}$$

MUDFLOW-2D is run using stored flow results so that it is possible to run many tides of the mud transport model using one tide of the flow model.

The fluid mud flow equations are solved as follows. The momentum equation in the x direction becomes:

$$u^{n+\frac{1}{2}}_{mij} = u^{n-\frac{1}{2}}_{mij} - \frac{g \Delta t}{\Delta x} (\eta^{n}_{i+1j} - \eta^{n}_{ij})$$

$$- \frac{g\Delta\rho \ \Delta t}{(\rho+\Delta\rho)\Delta x} (\eta^n_{mi+1j} - \eta^n_{mij} - \eta^n_{i+1j} + \eta^n_{ij})$$

+ source terms

and similarly for the y direction. This is essentially the technique used in explicit flow modelling but the free surface elevation η is now prescribed and only the fluid mud surface elevation η_m is calculated.

The fluid mud layer depth d_m can then be calculated as:

$$d^{n+1}_{mij} = d^n_{mij} + \frac{(F^{n+\frac{1}{2}}_{mxi-1j} - F^{n+\frac{1}{2}}_{mxij} + F^{n+\frac{1}{2}}_{myij} - F^{n+\frac{1}{2}}_{myij-1})}{\Delta x \Delta y} + \text{source terms}$$

where F_{mx} is the fluid mud flux in the x direction. Because of the steep bed slopes it was found to be best to compute F_{mx} as:

$$F^{n+\frac{1}{2}}_{mxij} = \Delta t \ \Delta y \ u^{n+\frac{1}{2}}_{mij} \ d^n_{mij} \qquad (u^{n+\frac{1}{2}}_{mij} \geqslant 0)$$

$$= \Delta t \ \Delta y \ u^{n+\frac{1}{2}}_{mij} \ d^n_{mi+1j} \qquad (u^{n+\frac{1}{2}}_{mij} \leqslant 0)$$

ie upstreaming on the depth of fluid mud in the cell. This ensures that if the fluid mud layer depth falls to zero in a cell then the corresponding flux of fluid mud out of that cell must also be zero.

This technique amounts to an explicit leapfrog scheme for the fluid mud depth. It has a timestep condition for stability but as it is a densimetric phenomenon the timestep criterion is much less stringent than in the flow calculation. In the case of the model of the Severn Estuary with a 500m grid it was found satisfactory to use a timestep of two minutes.

4 OBSERVATIONS OF FLUID MUD IN THE SEVERN ESTUARY

In the early 1970's the Institute of Oceanographic Sciences at Taunton carried out a field study of the occurrence of fluid mud layers in the Severn Estuary and the Bristol Channel, which is a prime example of a high energy turbid estuary. Kirby and Parker (Ref 4, 1973) described how on neap tides a large proportion of the mud in the Severn Estuary and Bristol Channel lies on the estuary bed as pools of stationary fluid mud. The fluid mud was described as ephemeral, being deposited as the tidal current energy decreased on the spring to neap cycle. They postulated that the fluid mud layers were formed by a process of deposition and by mud flowing from adjacent areas. The fluid mud was identified on 30, 150 and 200kHz echosounders as a ghost echo overlying the sea bed.

Settled mud deposits are of very limited extent in the Severn Estuary Fig (1). The channels are mainly rock floored and the subtidal banks are composed chiefly of rock with thin veneers of sand. The most extensive mud deposits are thick laminated gray clays which occur in Bridgwater Bay and Newport Deep, whilst other mud deposits occur along much of the shoreline.

Kirby and Parker found highly ephemeral layers of fluid mud in Swansea Bay, Cardiff Channel and in the approaches to Bridgwater Bay. The deep channels in the axis of the Bristol Channel below Holm Islands were not sites of fluid mud layers. Very large pools of fluid mud were found overlying settled muds in Newport Deep, whilst the largest and most persistent occurrences of fluid mud were found in the main channel between Clevedon and in the Shoots channel where it overlay rock or sand.

Kirby and Parker found fluid mud forming most rapidly as spring tides became neap tides. No fluid mud was found at Avonmouth on a 13m tide. However, the echosounder was incapable of detecting fluid mud layers less than about 0.25m thick (Ref 4). On a 10.5m tide small pockets of fluid mud were found. On 8 to 7m neap tides thick fluid mud layers were present at Avonmouth. They reported mud pools up to 5m thick in the Shoots Channel but they did not mention the mud concentrations. On the smallest equinoxial neap tides of about 5m range fluid mud was observed to form as far downstream at Clevedon (Fig 2).

The most ephemeral fluid mud layers were those observed in the Avonmouth area, where layers 3m thick were recorded at high water. The newly formed fluid mud layers were reported to have a homogeneous density.

The Port of Bristol Authority surveys detected stationary fluid mud suspensions in the vicinity of Avonmouth for a period of 3-4 days during neap tides with a range of about 7m.

In Newport Deep fluid mud 0.5 - 1.5m thick was reported to be stable during tides with a 6m range. The layers were not present during 13m tides.

Stationary suspensions were less frequently observed, and reached only 0.5m thick in Bridgwater Bay, mud was occasionally found in Holms channel but it was never observed in the area west of Flat Holm or near Culver sand.

Kirby and Parker demonstrated that the mass of suspended mud in the water column at high water was not sufficient to account for the thickness of the fluid mud layers in the deep channels. They therefore postulated the existence of density currents carrying fluid mud into the pools in the deep channels.

Density and mobility of the fluid mud

The fluid mud was identified as ghost echos on 30, 150 and 200kHz echosounders. Samples from the mud pools were obtained with a sample bottle which was triggered at the require depth from the surface by a messenger. The concentrations in the mud pools varied from as low as 4000ppm to as high as 440,000ppm. Kirby and Parker used a value of about 10,000ppm to define fluid mud but with no higher limit. Later in-situ measurements made by Kirby and Parker (Ref 5) with a gamma-ray transmission density probe showed that the stationary suspensions had a surface density of about 1.05T/m^3 and a layered structure with a wide range of much higher densitites. Odd and Rodger define fluid mud as having uniform concentration of about 75,000ppm, equivalent to a bulk density of 1.07 t/m^3 in seawater with a salinity of 28ppt.

Kirby and Parker reported that the most transient (young) slackwater layers of fluid mud had a uniform density, which appears to agree with the basic assumption in the theory described in this report. However, the samples collected by Kirby and Parker from the stationary pools of fluid mud in the deep channels on neap tides indicated that the mud had an average dry density of about 0.17 Tonnes/m^3 which Odd and Rodger define as a weak soil with a very much higher yield strength than mobile fluid mud. The theory described in this report assumes that fluid mud with a concentration of about 75,000ppm at rest dewaters to form a weak soil with a dry density of about 0.17 Tonnes/m^3.

It appears that the mud pools located by Kirby and Parker on small neap tides consisted of a low density fluid mud, overlying a weak muddy soil with a dry density of about 0.17 Tonnes/m^3. It is not clear whether the hydrostatic force exerted by the water surface slope at the main run of small neap tides is sufficient to shear the high density mud layers at the rock base. Instead, these denser layers may remain stationary and be eroded from the surface downwards.

Besides the deep pools of mud in the channel, Kirby and Parker reported the occurrence of small highly ephemeral (slackwater) deposits of fluid mud in the lower estuary. Such thin layers are not easily identified on an echosounding trace. However, the model described in this report postulates that ephemeral deposits of fluid mud will form almost anywhere in the Severn Estuary during the slackwater period if the rate of settlement of mud from suspension onto the bed exceeds the rate of which fluid mud dewaters.

5 SIMULATION OF FLUID MUD IN THE SEVERN ESTUARY

The new modelling method was used to set up a pilot model of mud transport in the Severn Estuary. The model was driven using stored tidal flow results from the depth-averaged model developed by HR for the Bondi study (Ref 2).

The Bondi model had three dynamically nested grids as shown in Fig 1: a 4500m grid from 5°W to 4°W, a 1500m grid from 4° to 3° 15' W, a 500m grid from 3° 15' W to the Severn Road Bridge and a one-dimensional model upstream of the Road Bridge. An isometric projection of the bathymetry of the 500m grid from SW of the Holm Islands to the Severn Road Bridge is shown in Fig 3

The model was calibrated to simulate conditions during a 13.3m spring tide (at Avonmouth) on 14 May 1980 and a 6.8m neap tide (at Avonmouth) on 22 May 1980 (Ref 2).

The main purpose of the exercise was to attempt to simulate the spatial and temporal patterns of the formation of fluid mud layers as observed by Kirby and Parker on spring and neap tides (Ref 4).

The fluid mud model was linked to a standard two-dimensional depth-averaged suspended mud transport model of the Severn Estuary. Once formed, the fluid mud layer was assumed to move under the action of gravitational, hydrostatic and frictional forces, without feedback on the motion of the overlying water.

Simplified initial and boundary conditions for the suspended mud concentrations were based on observations (Refs 5-7). The average observed suspended mud concentrations at the surface (a) and bed (b) on a spring tide are shown in Fig 4 (Ref 6). The blank areas were not sampled. The two-dimensional depth-averaged mud transport model was assumed to have an initial uniform concentration of suspended mud of 5,000ppm and 3,000ppm within the area of the 500m grid (3° 15m West to the Severn Bridge) on 13.3m spring and 6.8m neap tides, respectively. The concentration of suspended mud passing seaward through the Shoots channel on the ebb tide was assumed to be the same as the initial values prescribed for spring and neap tides, namely 5,000ppm and 3,000ppm, respectively. Observed mud concentrations in the Shoots on a spring tide are shown in Fig 5.

The concentrations of suspended mud at the seaward end of the model was assumed to be zero on the incoming tide. The models were run for a few repeating semi-diurnal tidal cycles.

The settling velocity of the suspended mud flocs at the base of the water column was assumed to be related to the depth-averaged suspended mud concentration as follows.

V_s (mm/s) = 0.005C ppm

The exaggerated value of the coefficient, which normally has a value of about 0.002, was necessary to compensate for the fact that the concentration of suspended mud near the bed is usually significantly higher than the depth-averaged values in the Severn Estuary.

This crude assumption for the settling velocity could only be avoided by using a full three-dimensional mud-transport model which is capable of reproducing the correct vertical concentration profiles Fig 6. The suspended mud was assumed to settle into the potential fluid mud layer when the bed stress calculated from the depth-mean tidal velocity fell below $0.4N/m^2$ (smooth bed). This was also a crude assumption. In reality, suspended mud would settle into the potential fluid mud layer when the flux of settling mud exceeds the vertical turbulent flux of mud. This condition could be simulated much more realistically in a three-dimensional model. The settled mud was assumed to be eroded after the fluid mud had been entrained into the overlying flow and when the bed stress exceeded $0.3N/m^2$, assuming a smooth mud bed.

The fluid mud was assumed to have uniform density, ($C_0 = 75kg/m^3$) ($\gamma_B = 1.066T/m^3$, $\gamma_W = 1.02$). The fluid mud was assumed to dewater when it was stationary at a rate of 0.05mm/s. The fluid mud was also assumed to have a Bingham lower yield shear strength of 0.1N/m^2.

The results from the interlinked models TIDEFLOW-2D, MUDFLOW-2D and FLUIDMUD-2D are presented in terms of spatial distributions of tidal velocity vectors, fluid mud velocity vectors, suspended mud concentrations and the thickness of the fluid mud layer at selected times in the tidal cycle. The results are also presented in terms of time histories of the same variables and tidal levels at selected positions in the estuary, namely 10A in Newport Deep, 11 in Bristol Deep, 11A in King Road, 11B on the Welsh Grounds and 12 in the Shoots channel as shown in Fig 7. The sites are numbered in accordance with the original simultaneous fixed stations observations made by HR in 1980 (Ref 7).

5.1 Spring tides

Conditions during a 13.3m tide (at Avonmouth) were simulated to investigate the possible occurrence and behaviour of thin fluid mud layers at slack water. This was done despite the fact that Kirby and Parker's echo sounding surveys showed no significant layers of fluid mud >0.25m on spring tides. Because previous research (Ref 1) has shown that suspended solids concentrations in the Severn Estuary during spring tides exceed 2500ppm just above the bed at slackwater, one should therefore expect a very wide occurrence of thin layers of fluid mud during the short period of slackwater at the change of tide.

It should also be noted that the thickest fluid mud layers form in the Parrett Estuary during spring tides when suspended solids concentrations are highest.

The predictions from the research models are extremely tentative due to the crudeness of the suspended transport model, the simplified initial and boundary conditions and the lack of knowledge of the optimum values of several empirical coefficients.

The calibration of the Bondi model showed that it simulated the vertical tide and the speed and direction of the depth-mean tidal currents at the positions shown in Fig (7) (Ref 2). It was therefore assumed that the depth-mean tidal velocities in the rest of the model were realistic. (Note that HR are presently constructing and re-calibrating a finer 250m gridded model of the estuary). The simulated spring tidal velocities at stations 10A, 11, 11A, 11B and 12 are shown in Fig 8, the corresponding spring tide curves at the same locations are shown in Fig 9. Note that the Welsh Ground dries out at a level of about -2m OD (N). The spatial distribution of depth-mean suspended mud concentrations at HW and LW on the first tide are shown in Figs 10 and 11, respectively. The concentrations are approximately similar to the tide-averaged distributions of bed and surface mud concentrations on spring tides in the Severn Estuary published by Kirby and Parker Fig 4. Note the canalisation of the turbid water discharged through the Shoots on the ebb tide into King Road and Bristol Deep.

The suspended mud concentrations decreased on subsequent repeating tides as shown in Fig 12. The excessive load of suspended mud prescribed initially by the uniform concentration of 5000ppm, settled over much of the estuary excluding the deep channels but including large areas which are normally sandy or exposed rock (Fig 1).

However, the pattern of suspended mud concentrations was considered to be adequate for initial investigations of the formation and behaviour of fluid mud at slackwater.

The initial runs of the model with very approximate coefficients simulated the growth of a thin fluid mud layer on the bottom of most of the deep channels at HW slack (Fig 13), which lasted for about one hour as shown in Fig 14 for selected sites whose locations are shown in Fig 7.

The fluid mud deposit was obviously formed directly from suspension and from the flow of fluid mud from the side slopes of the channels as shown by the pattern of fluid mud velocity vectors in Fig 15. The fluid mud could only exist for a short period when the bed stress falls to very low values near slack water (Fig 14).

The model predicted a much patchier distribution of fluid mud at low water with much less in the Bristol Deep and more in the vicinity of Steep Holme, Fig 16. The model results were extremely sensitive to the critical value of the bed stress at which suspended mud was assumed to settle into the fluid mud layer.

The main finding from this simulation appears to be the possible importance of the lateral flow of fluid mud from the shallows into the deep channels at the slack water periods. The component of gravity down the sloping channel banks is the main mechanism causing this motion. It is also possible that the fluid mud is re-eroded much more rapidly by entrainment than it would be possible to re-erode a settled mud bed by surface erosion. So although the fluid mud appears to play a relatively minor role in the pattern of mud transport on spring tides in the Severn Estuary, it may be effective at concentrating the mud in the deep channels on the English side of the estuary and in maintaining the extremely high mobility of this suspended load.

5.2 Neap tides

Conditions during a 6.8m neap tide were simulated by prescribing an initial concentration of suspended mud of 3000ppm and a similar concentration of mud in the ebb flow discharging through the Shoots channel. This concentration agreed approximately with observations made by Kirby and Parker (Ref 5) and with observations made by HR on 19 August 1980, Ref 7.

The simulated tidal velocities at stations 10A, 11, 11A, 11B and 12 are shown in Fig 17. The simulated suspended mud concentrations at the same sites are illustrated in Fig 18. A pattern of mud concentration appears to almost repeat each tidal cycle. The concentrations of mud on the Welsh Grounds (station 11B) were significantly lower than in the Bristol Deep (station 11). The model predicted relatively thick layers of fluid mud with a concentration of about 75000ppm would form in the Shoots channel, King Road, Bristol Deep, Newport Deep and even further down stream (Figs 19, 20 and 21). The fluid mud existed for more than 3 hours at low water slack in Newport Deep (station 10A) reaching a thickness of about 0.6m. The fluid mud was nearly 1m thick in Bristol Deep (station 11) and in the Shoots channel (station 12), where it occurred for about 2 hours at high and low water slack. The occurrence of fluid mud at the selected sites (Fig 21) coincided with periods when mud was settling rapidly from the overlying water (Fig 18). No fluid mud was formed on the Welsh Grounds at high water (station 11B).

There was evidence that the fluid mud flowed into the deep channels from the side slopes, Figs 22 and 23, and backwards and forwards along the channels at velocities of up to 0.3m/s, one hour either side of slack water (Fig 24). However, the direction of flow of the fluid mud did not correspond exactly with the direction of the overlying water. (Figs 22 and 23).

The pattern of fluid mud deposits more or less agreed with the observations of mud pools observed by Kirby and Parker shown in Fig 2. The big discrepancy between the observed and computed depths of the fluid mud layers may be explained in part by the fact that the echo sounder could not distinguish between fluid mud with a density of about 1.07 and new low density settled mud with a density of about 1.2 t/m^3.

The main finding from the neap tide simulation appears to be the possible importance of the large quantities of mud along the deep channels within the ephemeral fluid mud layers. The hydrostatic force due to the water surface slope, and not the slope of the bed is probably the main mechanism for moving the fluid mud along the channels. Evidence for this is the fact that the direction of movement of the fluid mud reverses at slackwater (Fig 24). The fluid mud ceases to move for a short period at slack water (Fig 24) when the applied forces are less than the lower yield strength of the mud, which is assumed to behave as a Bingham fluid.

6 DISCUSSION AND CONCLUSIONS

The modelling exercise showed that it is possible to simulate the main processes causing the growth, motion and re-entrainment of ephemeral fluid mud layers in a high energy turbid estuary like the Severn Estuary.

The main processes are:

Settlement of suspended mud into the lower layers of the flow as the vertical turbulent flux decreases near slackwater.

A negligible or very slow rate of dewatering of the fluid mud.

Flow by gravity down the sloping bed into deep channels.

Flow along deep channels under the action of hydrostatic forces generated by the slope of the water surface.

Entrainment by the overlying flow.

The main findings appear to be:

The importance of the lateral flow of fluid mud from the side slopes concentrating the mud in the deep channels located mainly on the English side of the estuary.

The manner in which fluid mud is rapidly re-suspended by the process of entrainment by the over lying water after slack water, thereby greatly increasing the mobility of the sediments.

The contribution that the mass movement of mud in the fluid mud layer makes to the total mud transport in the estuary.

The main weaknesses of the modelling techniques are:

The lack of resolution of the suspended mud concentration profile in a 2-dimensional depth-averaged mud transport model.

The lack of firm field evidence that fluid mud behaves as a Bingham fluid with a lower yield strength. The present value of $0.1N/m^3$ is based on rotating viscometer measurements made in 1962 (Ref 1).

The lack of evidence for defining the rate of dewatering of fluid mud, which is at present based on a single laboratory measurement made with clay in fresh water (Ref 1).

The lack of evidence that the fluid mud is entrained in a similar manner to salt in a stationary saline wedge.

The lack of field observations which are capable of separating mobile fluid mud with a density of about 1.07 Tonnes/m^3 and a stationary low density soil with a density of about 1.2 Tonnes/m^3.

The proposed modelling method cannot be used to make firm predictions of the effects of engineering works on mud transport in turbid high energy estuaries until there is more solid evidence and justification for some of the basic assumptions and the values of the coefficients described in this report. At its present stage of development the modelling method can only be applied to make a preliminary assessment of the importance of fluid mud in maintaining the pattern of mud transport and siltation in a particular estuary.

The new modelling method could be refined into a tool capable of solving practical engineering problems if the following research and development was carried out.

i) make detailed observations in the Parrett Estuary to evaluate the shear stress at which fluid mud starts and stops moving along a channel bed and hence determine its Bingham yield strength.

ii) conduct new laboratory experiments to determine the rate of dewatering of fluid mud in seawater and its rate of entrainment by an overlying layer of clear water.

iii) deploy density probes to map out the distribution, thickness and density of fluid mud layers in the Severn Estuary.

iv) Link the new fluid mud model to a standard three-dimensional suspended mud transport model.

7 REFERENCES

1 Odd N V M Odd and Rodger J G. An analysis of the behaviour of fluid mud in estuaries. Hydraulics Research Report SR 84, March 1986.

2 Hydraulics Research Ltd. Severn Tidal Power. Two-dimensional water movement model study Report EX 985 July 1981.

3 Hydraulics Research and saline intrusion and sediment transport in the Rotterdam waterway - HR Report EX 883, September 1979.

4 Kirby R and Parker W R. Fluid mud in the Severn Estuary and Bristol Channel and its reference to pollution studies. The Institution of Chemical Engineers Symposium on Estuarine and Coastal Pollution, Sept 1973.

5 Kirby R and Parker W R. Distribution and Behaviour of fine sediment in the Severn Estuary and Inner Bristol Channel Can.J.Fish Aquat. Sci. 50 (suppl 1) 83-95 (1983).

6 Kirby R and Parker W R. A suspended sediment front in the Severn Estuary. Nature Vol 295. No 5848 pp396-399 4 Feb 1982.

7 Hydraulics Research. The Severn Estuary, observations of tidal currents, salinities, solids HR Report EX 966 Jan 1981.

FIGURES.

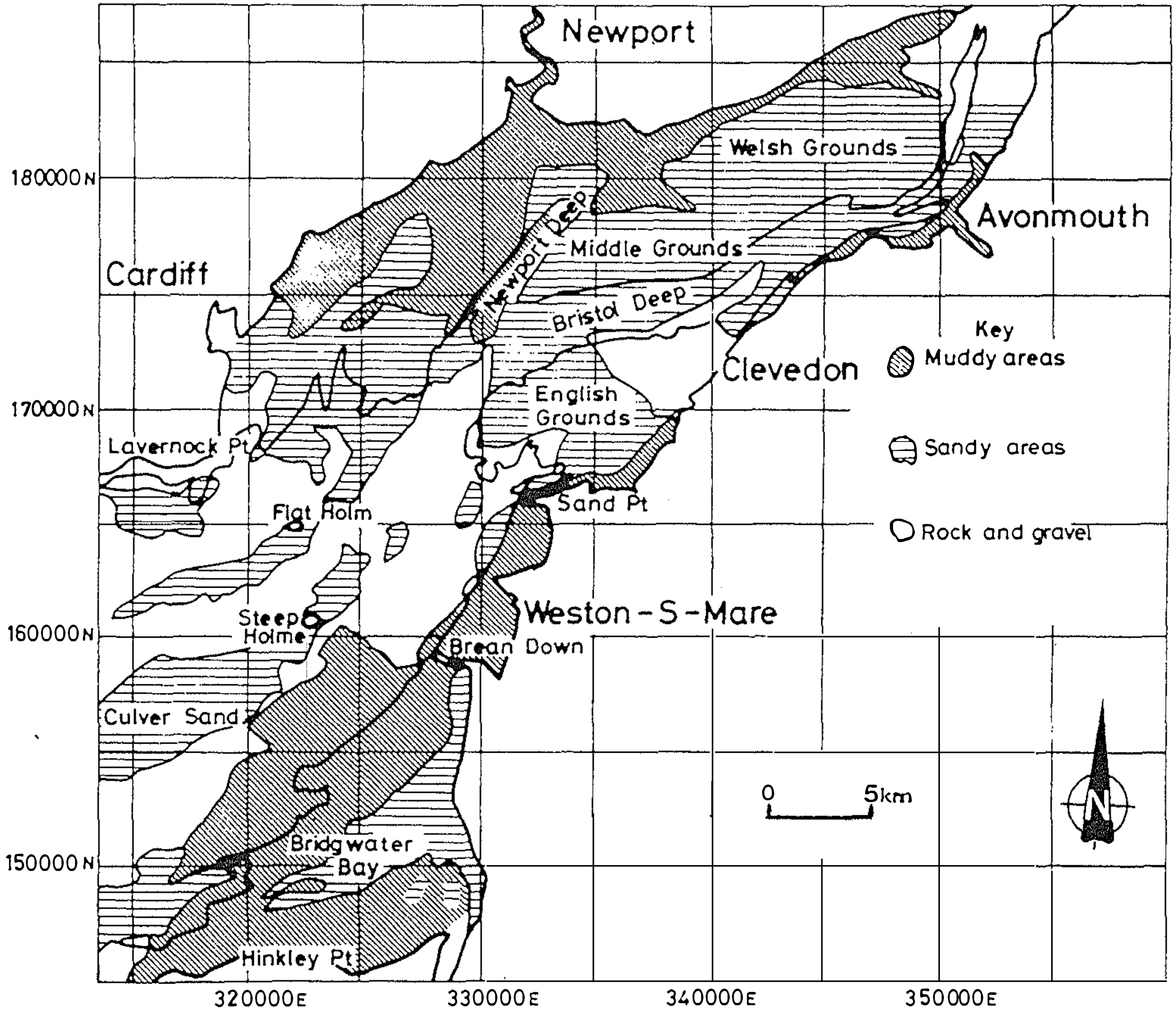

Fig 1 Location plan and distribution of bed surface sediment in the Severn Estuary.

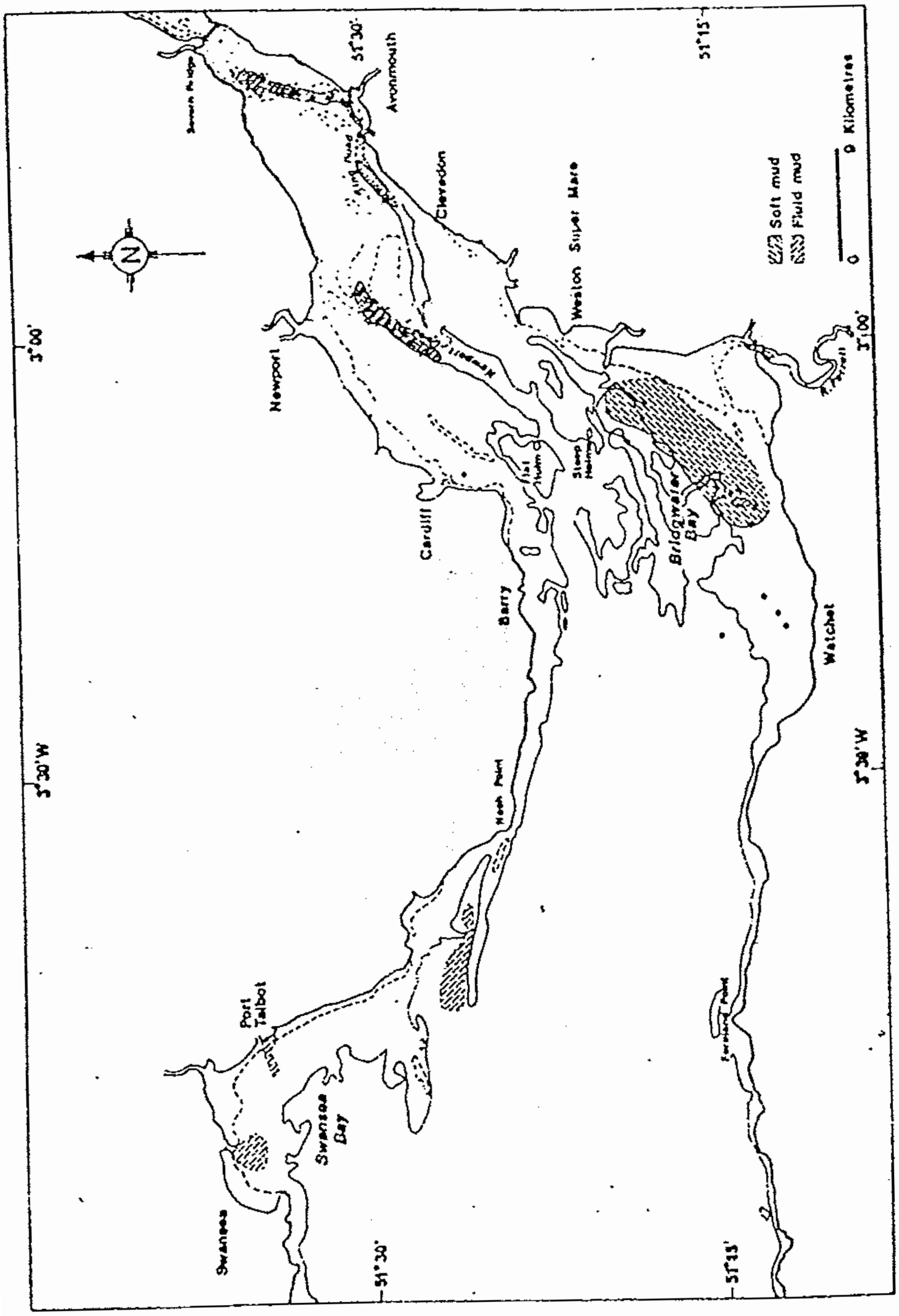

Fig 2 Location of fluid mud pools and soft mud in the Severn Estuary (after Kirby and Parker, 1973).

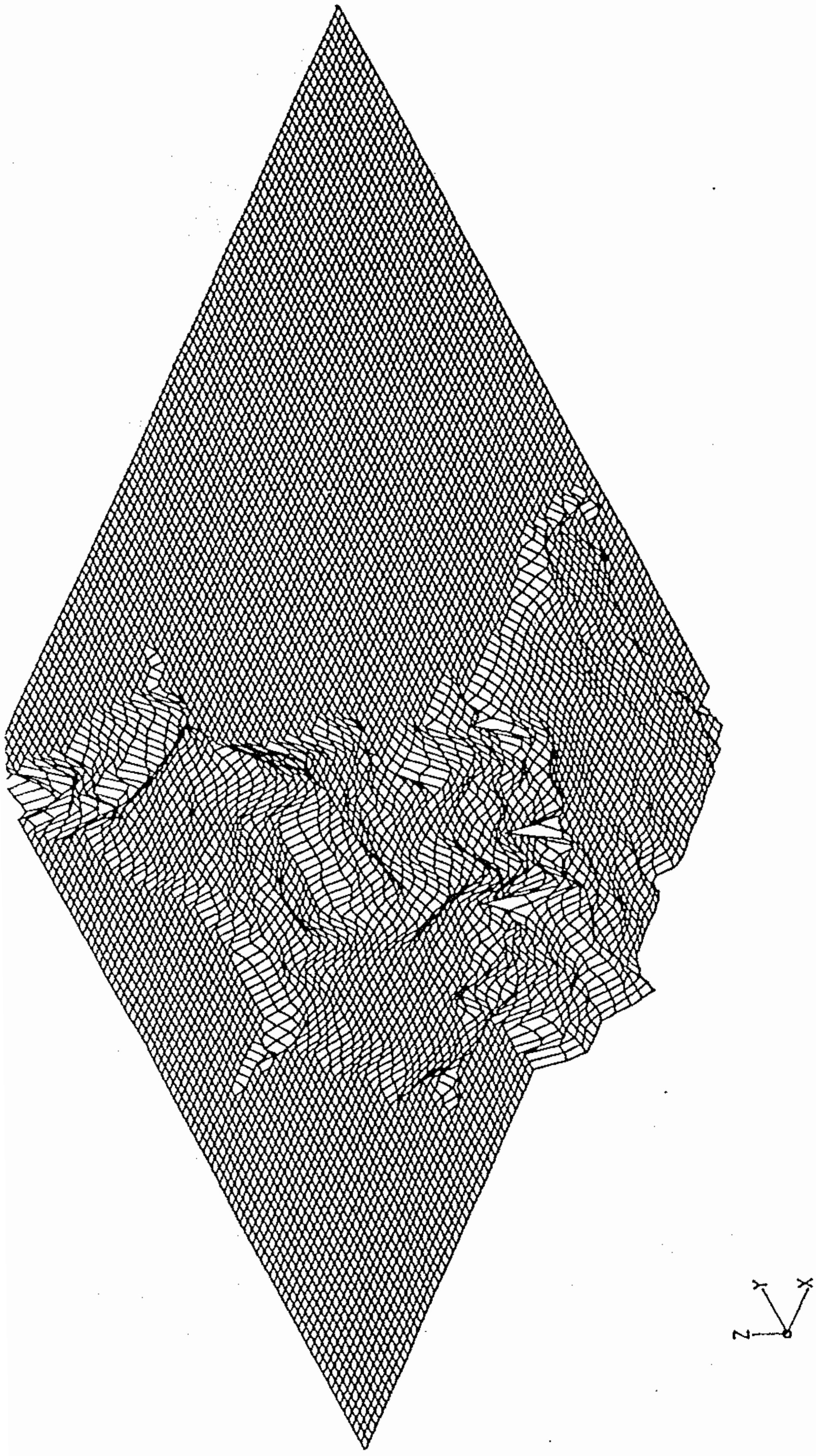

Fig 3 Bathymetry of the Severn Estuary Bondi Model from 3°15'W to the Severn Road Bridge.

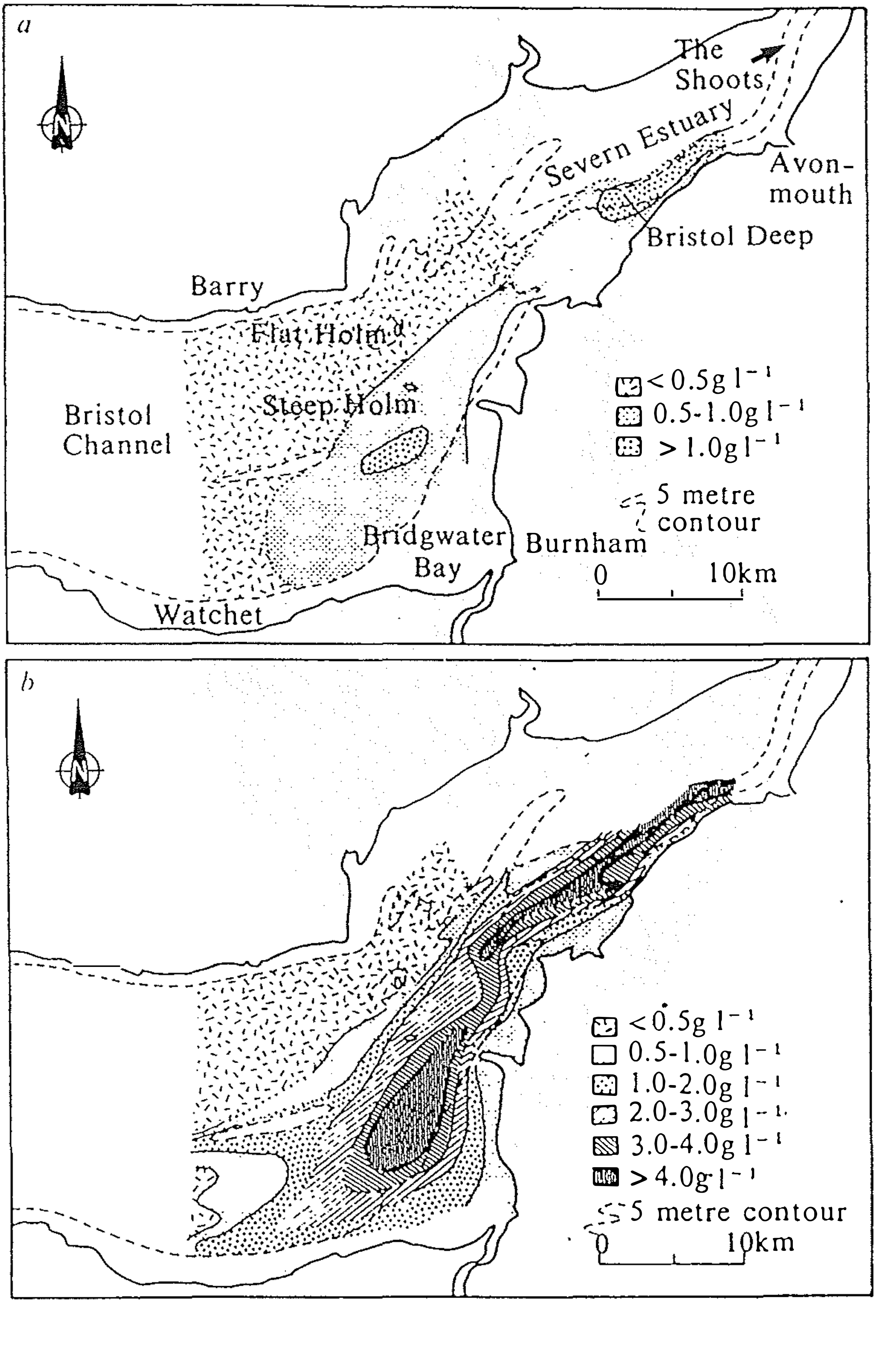

Fig 4 Averaged observed suspended mud concentrations on a spring tide (after Kirby and Parker, 1982).

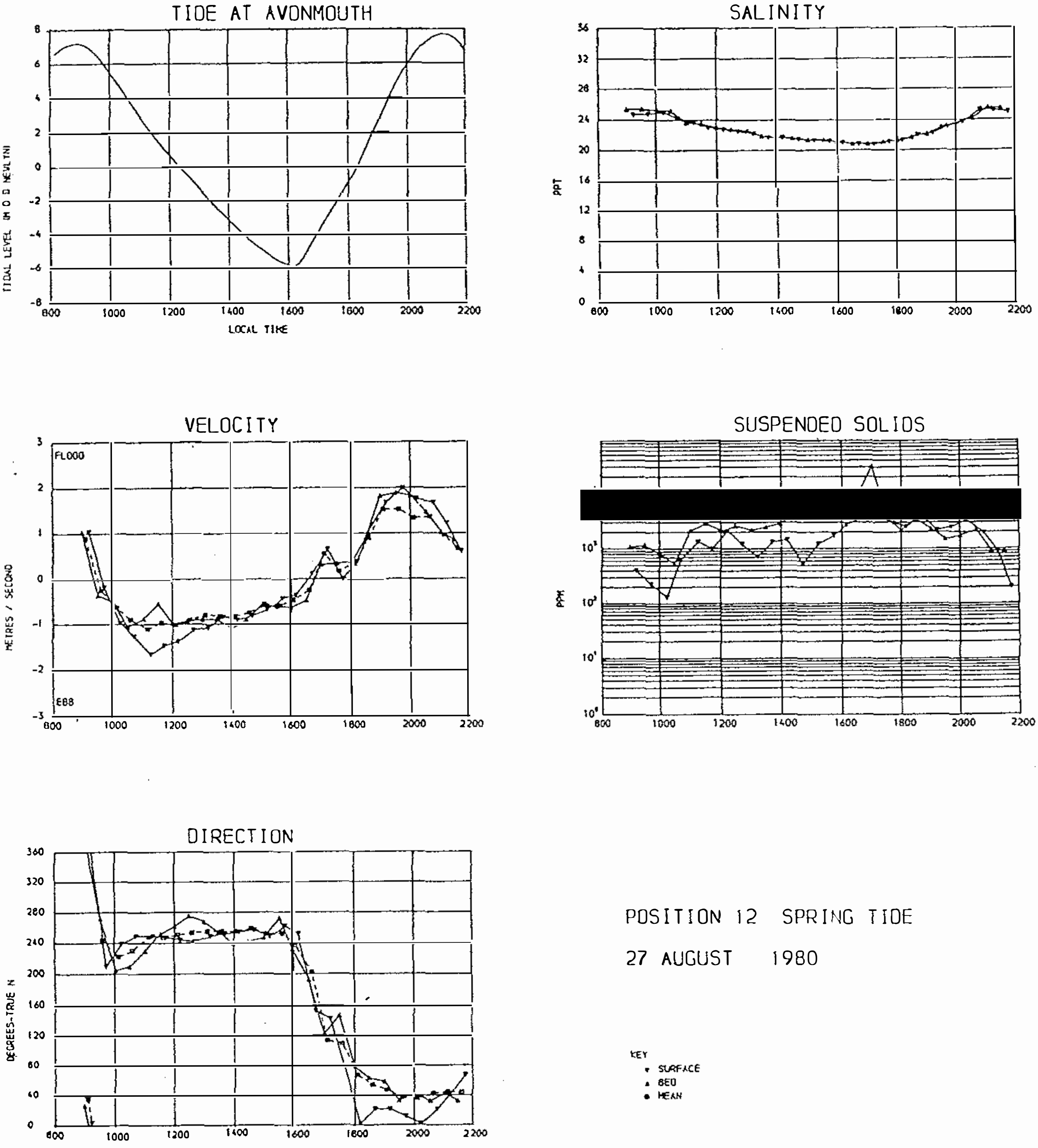

Fig 5 Observations of tidal currents, salinities and suspended mud concentration in the Shoots ; spring tide.

Fig 6 Mud concentration profiles in Bristol Deep on a spring tide.

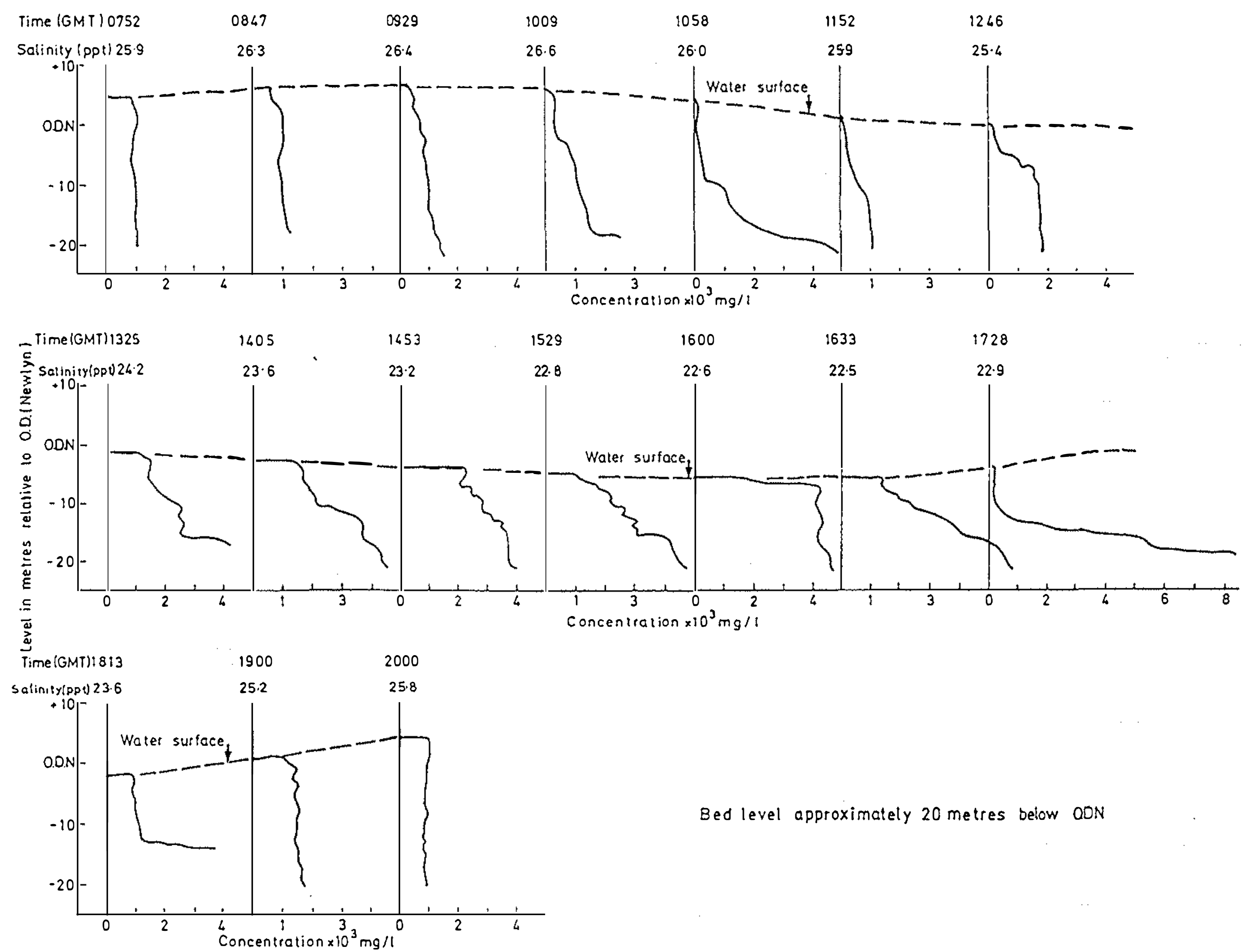

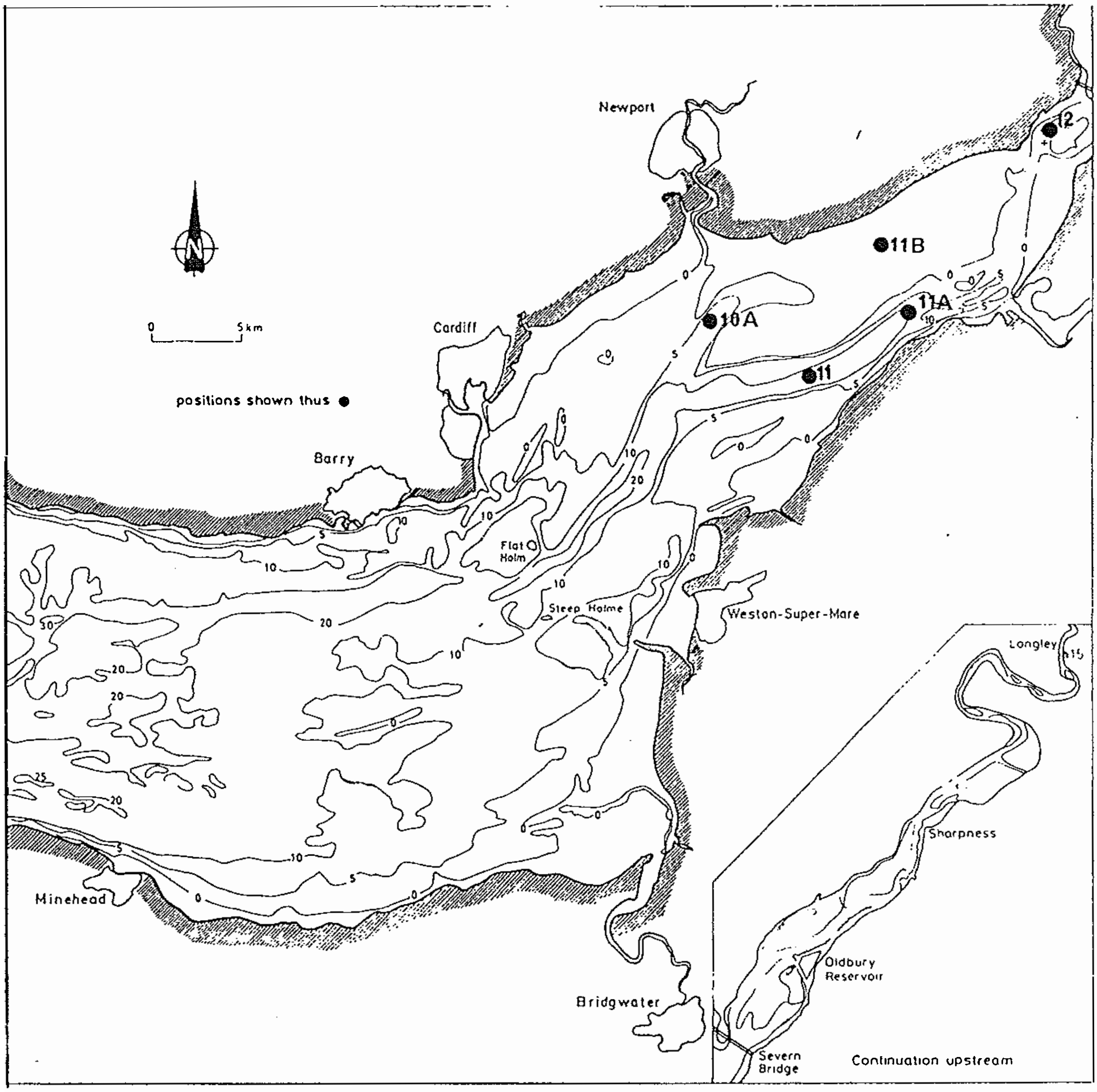

Fig 7   Locations for which model results are presented.

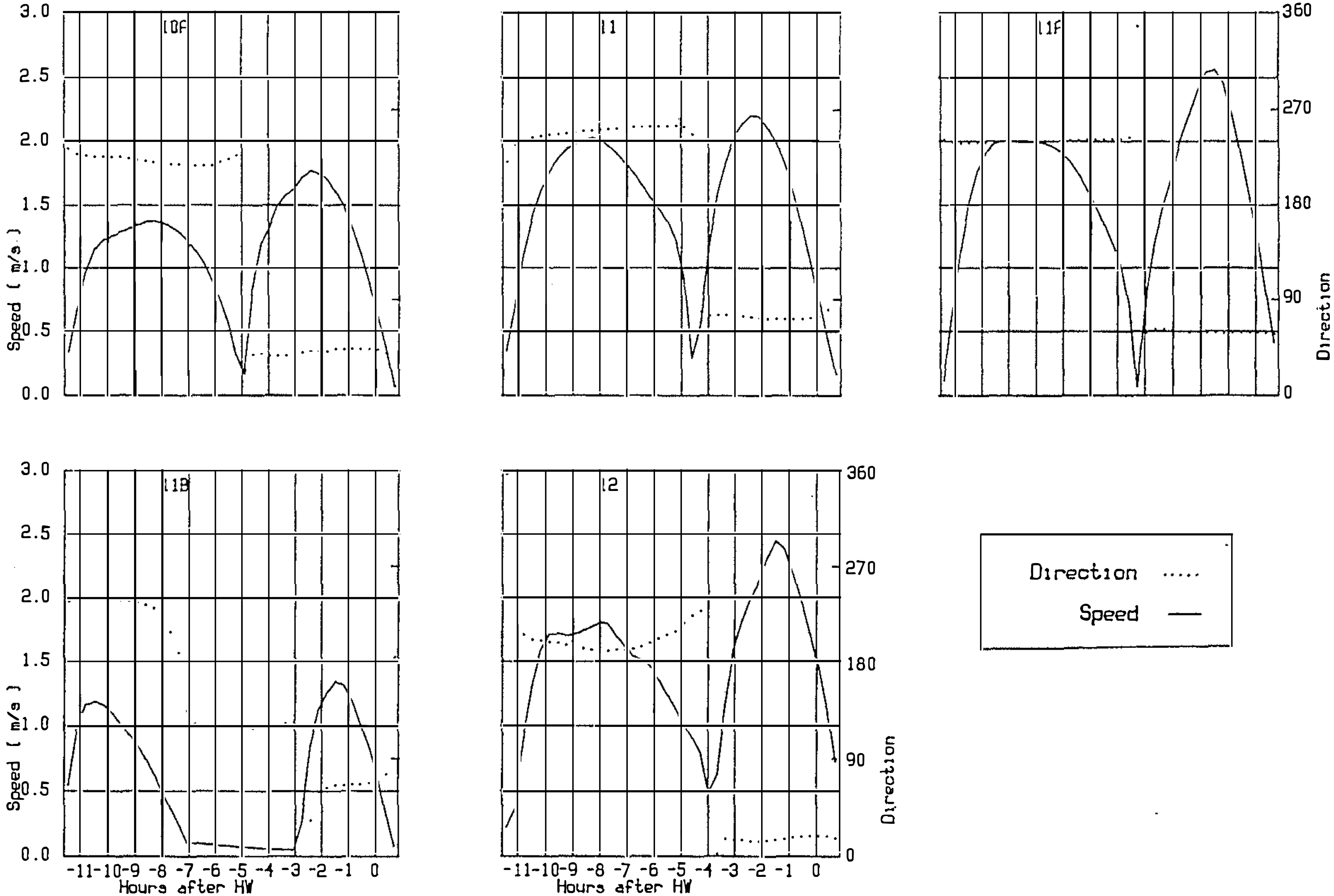

Fig 8 Simulated spring tide velocities -Bondi model.

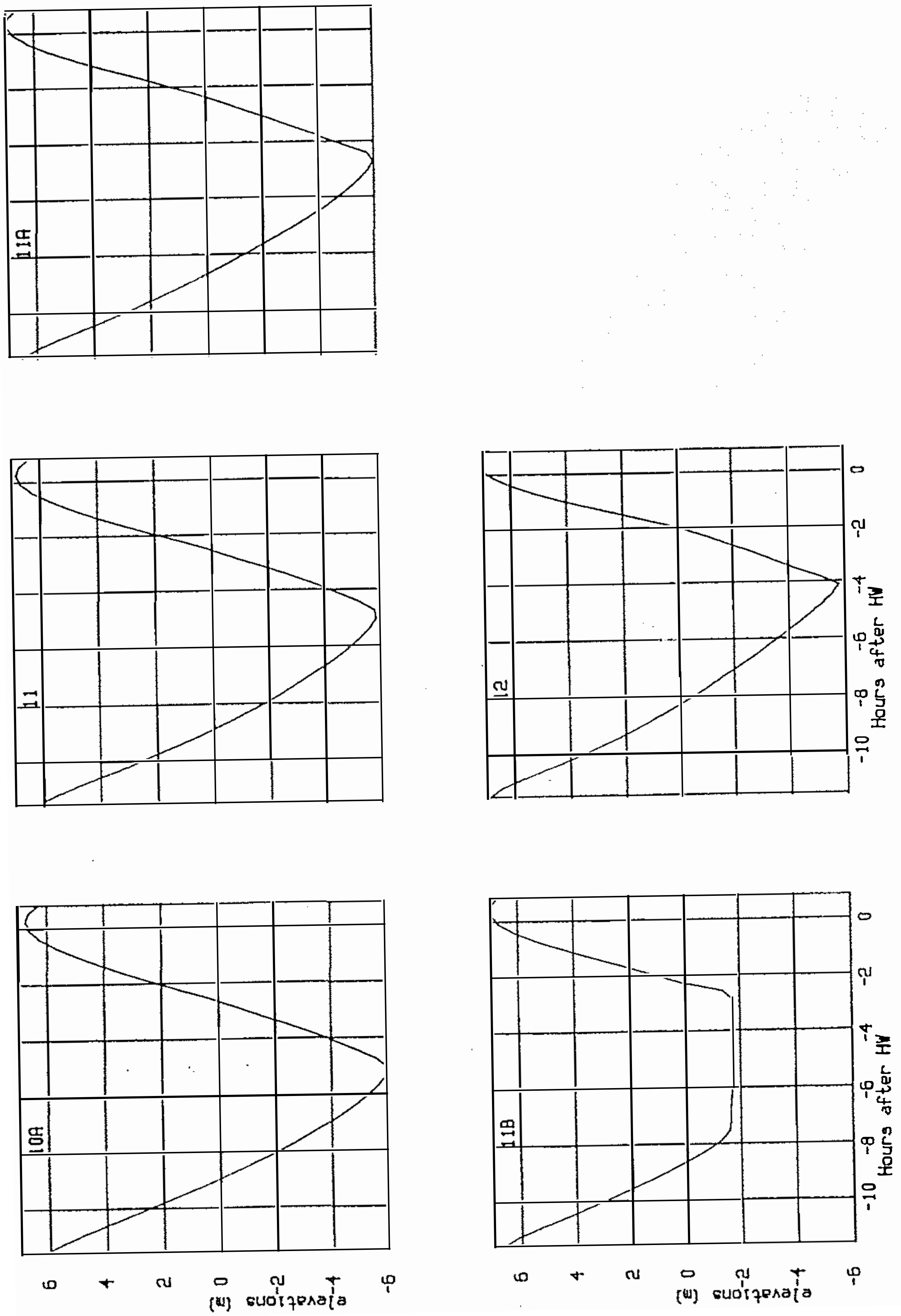

Fig 9   Simulated tidal elevations
-Bondi Model.

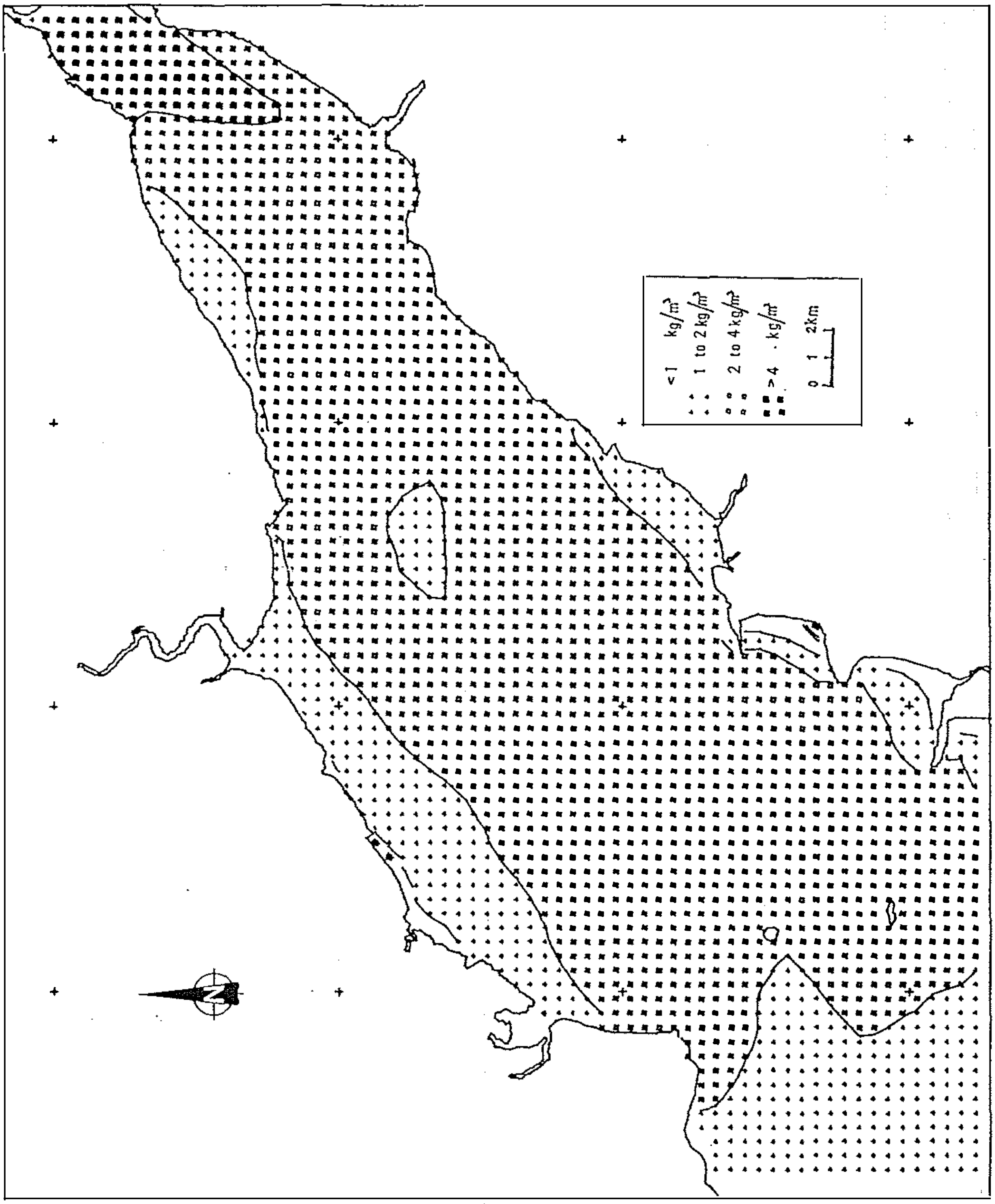

Fig 10 Simulated depth-averaged suspended mud concentration-HW spring tide.

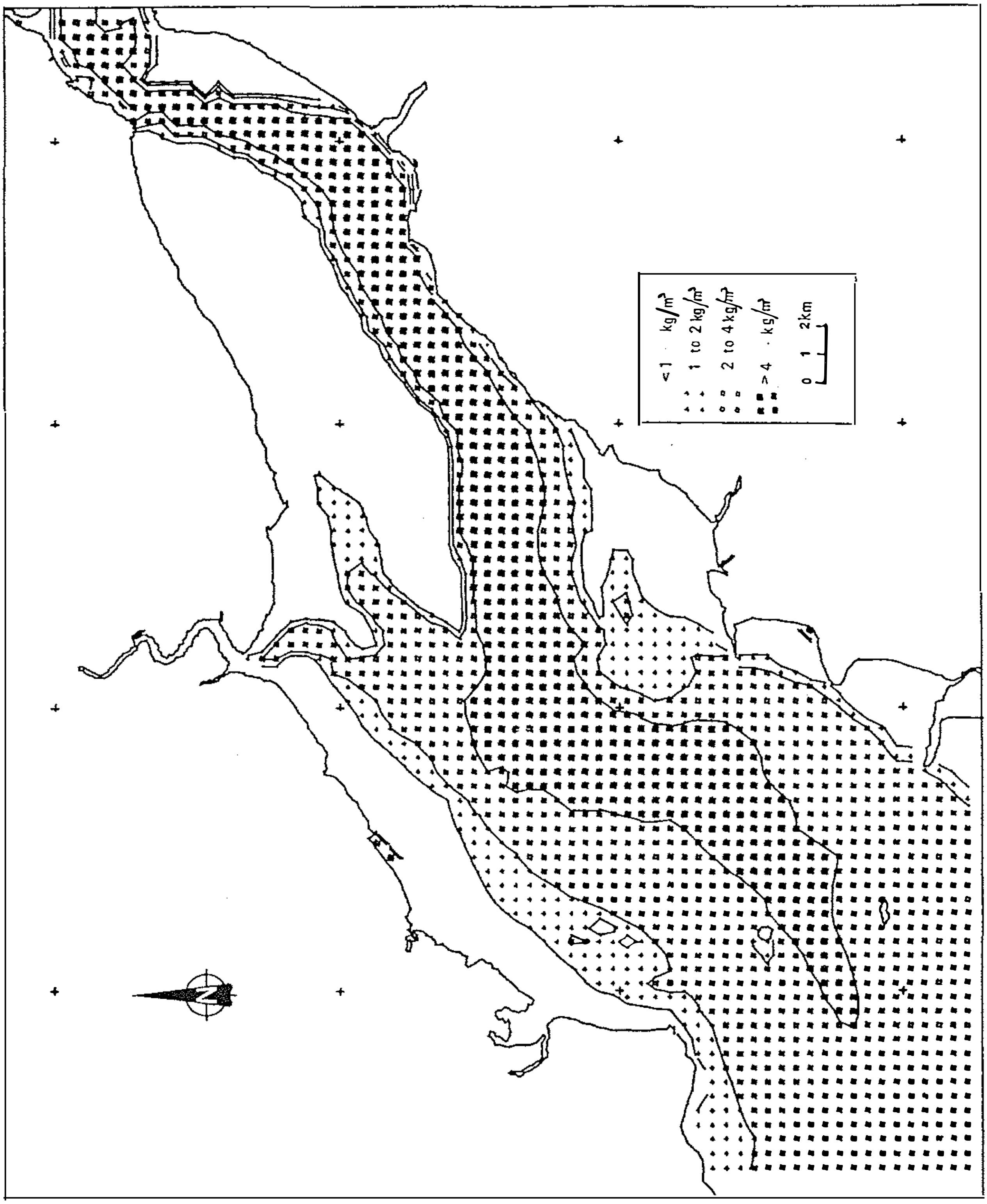

Fig 11 Simulated depth-averaged suspended mud concentration-LW spring tide.

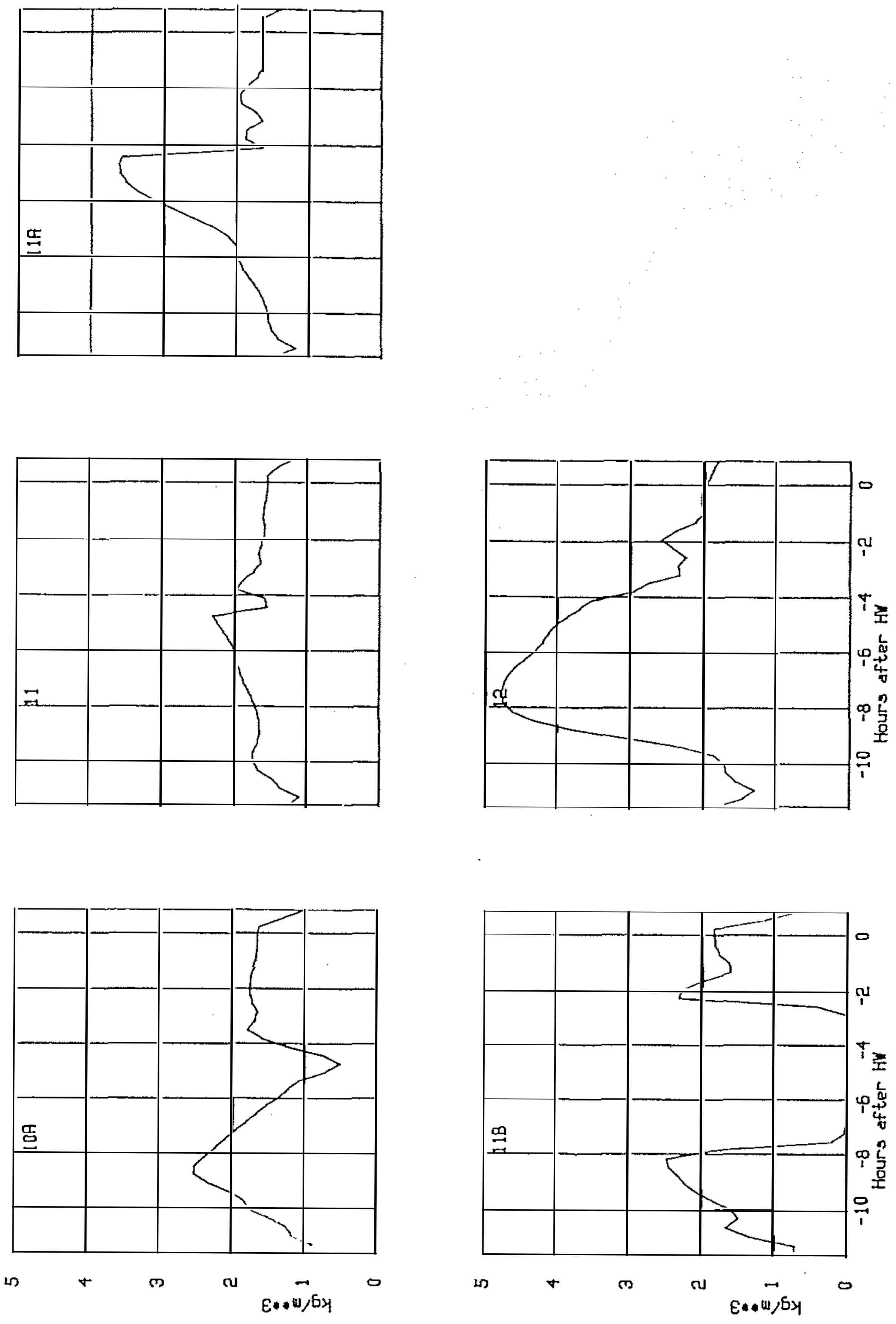

Fig 12 Simulated suspended mud concentration
after several tidal cycles

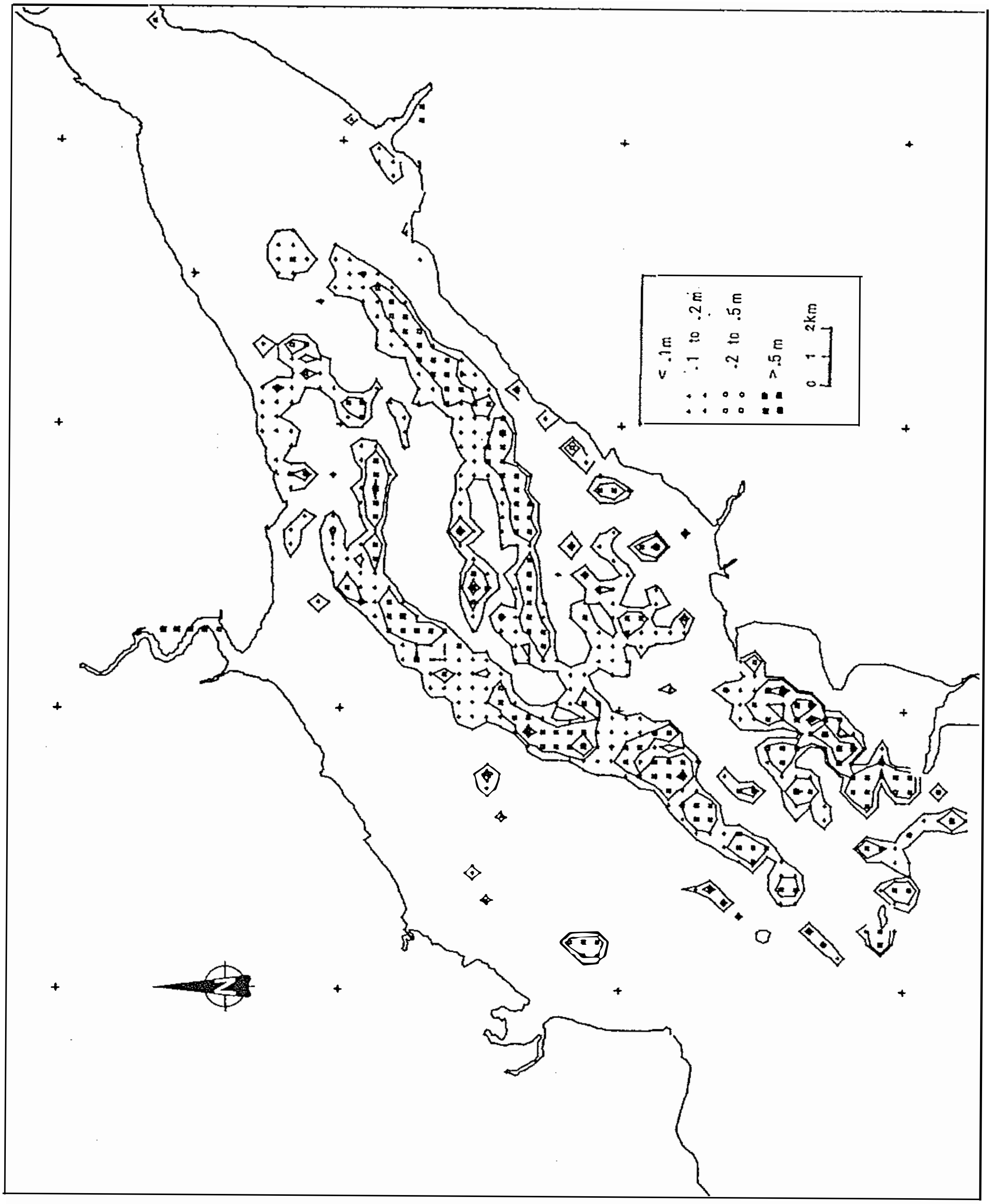

Fig 13 Simulated distribution and depth of
fluid mud layer at HW slack spring tide.

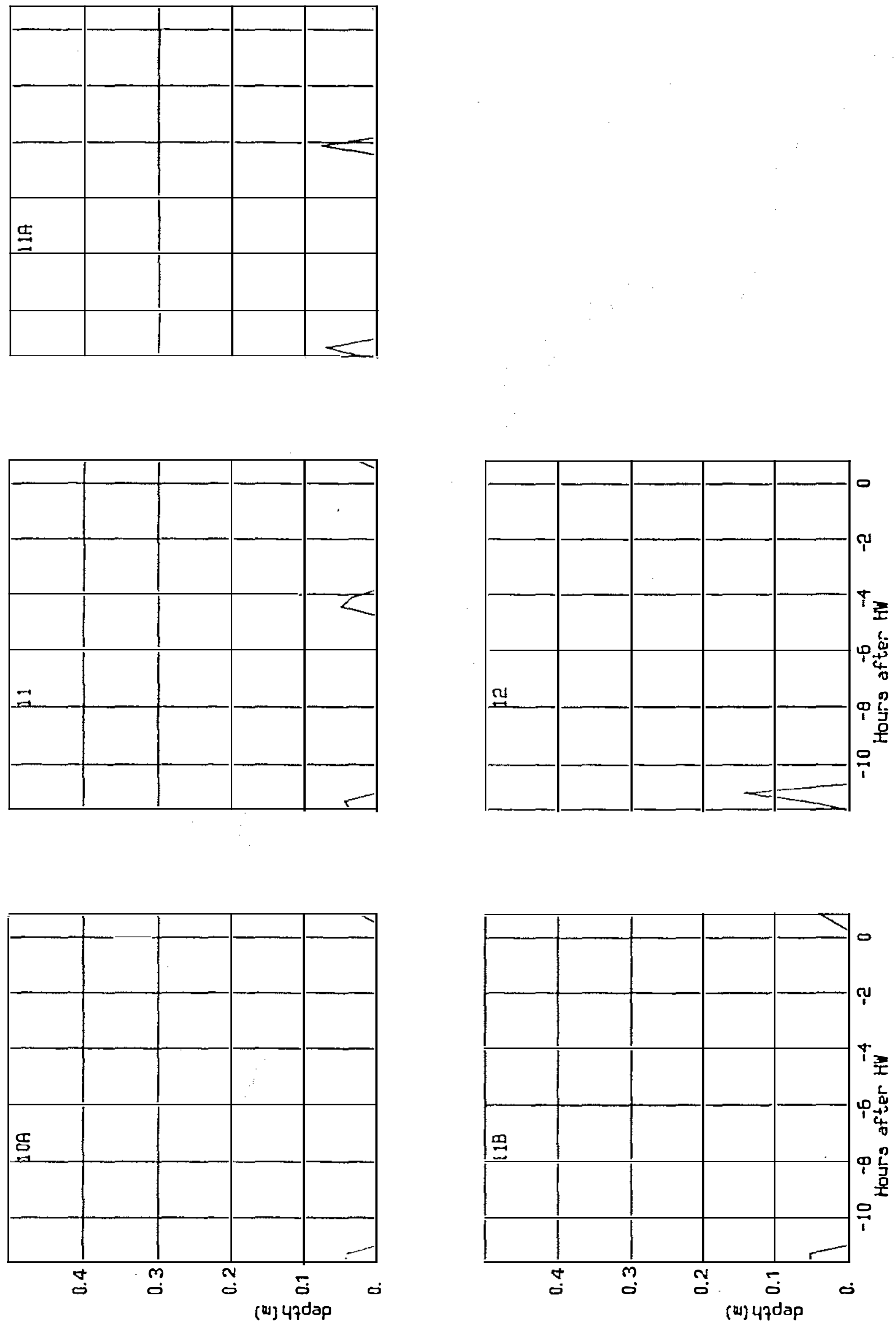

Fig 14 Simulation growth and entrainment of fluid mud layer at spring tide.

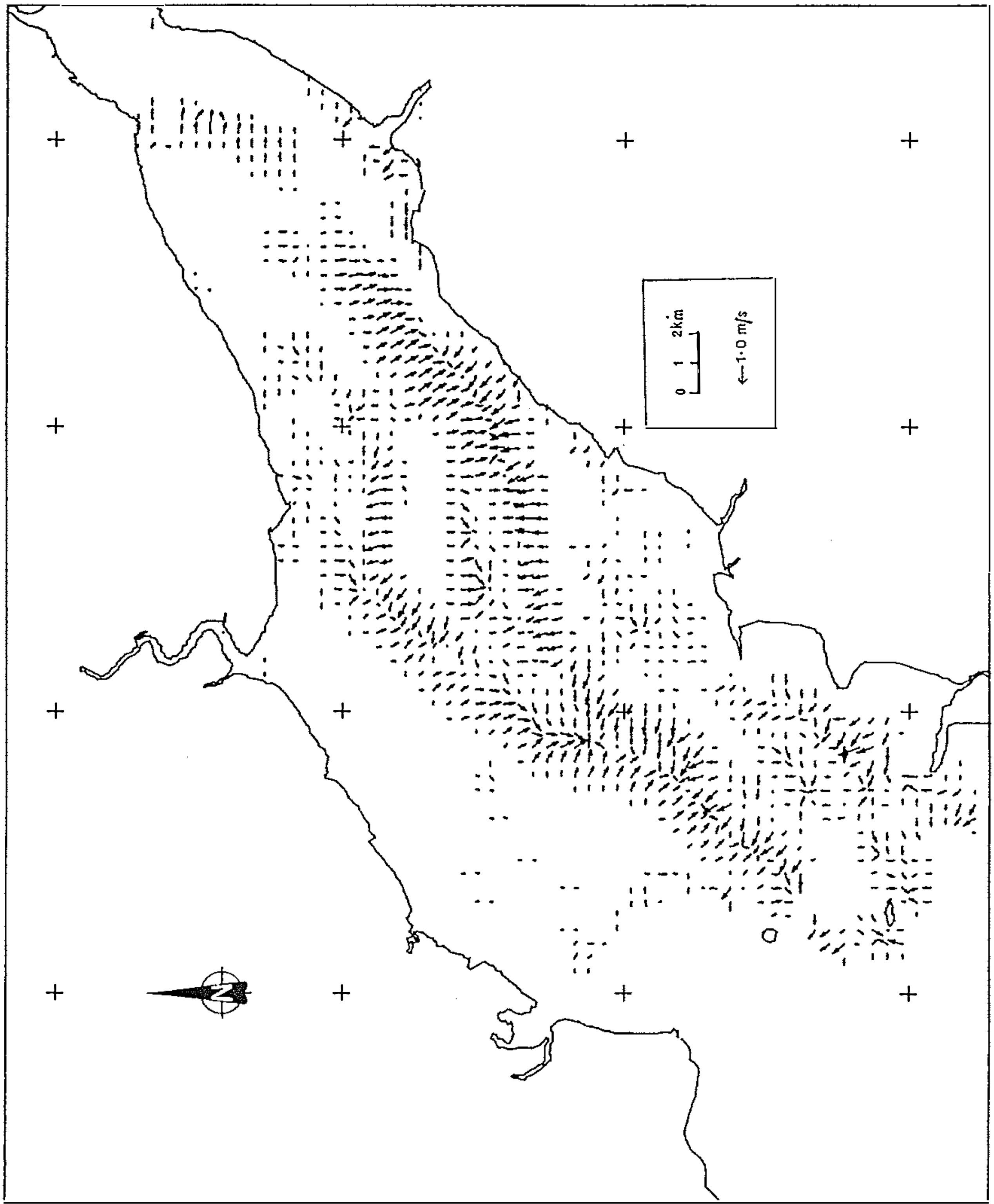

Fig 15 Simulated fluid mud velocity vectors at
HW slack spring tide.

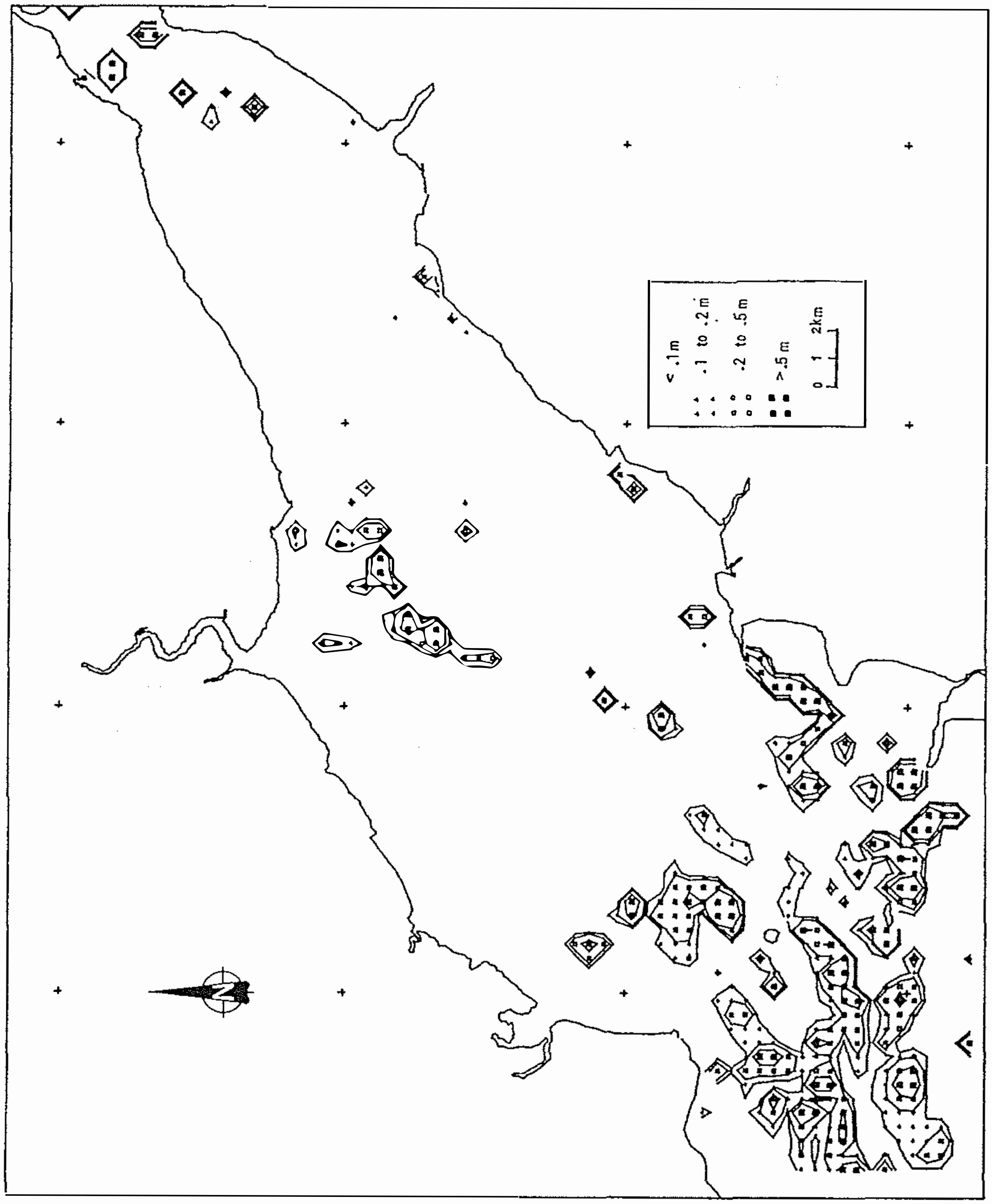

Fig 16 Simulated distribution and depth of fluid mud layer at LW slack spring tide.

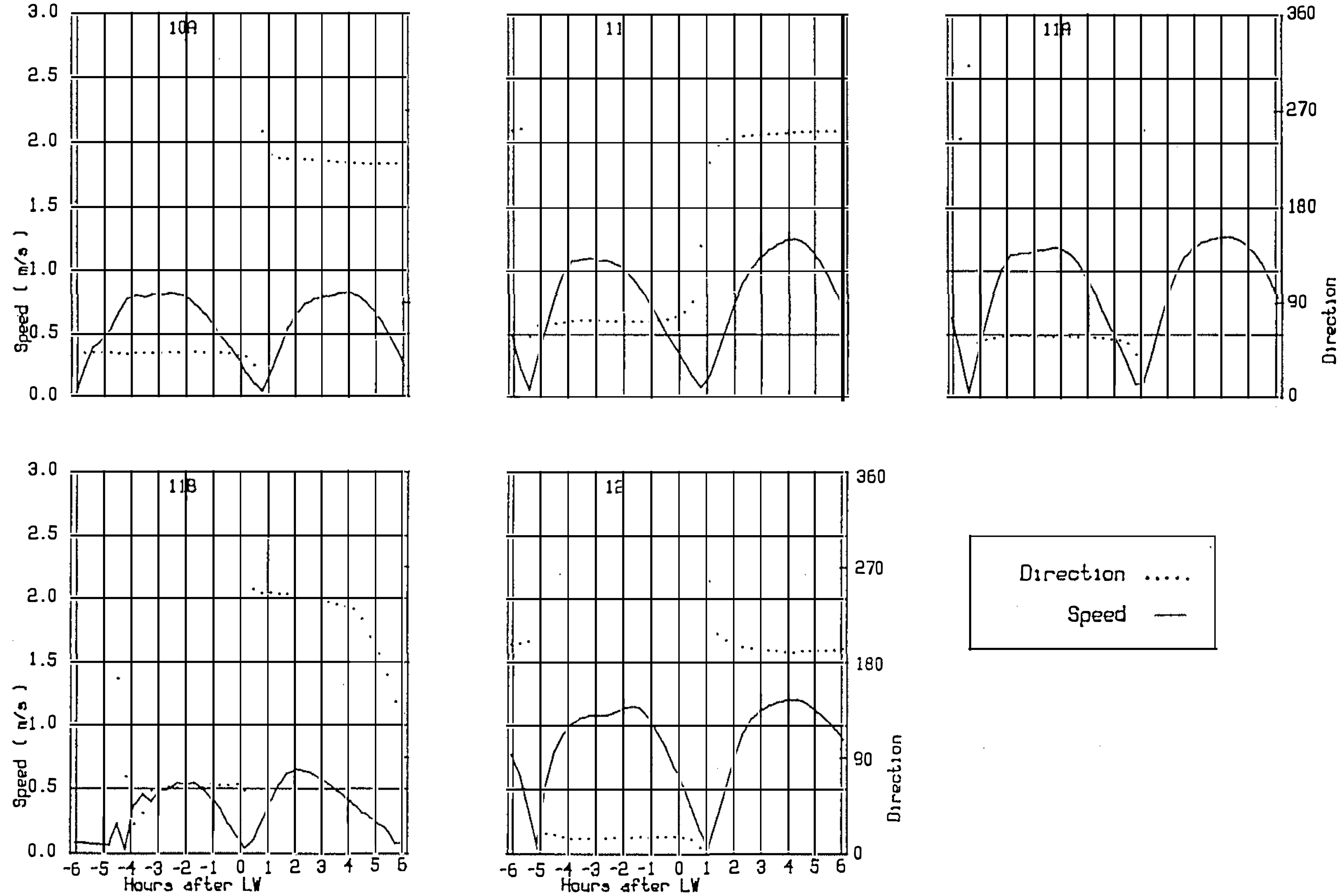

Fig 17 Simulated neap tide velocities
-Bondi Model

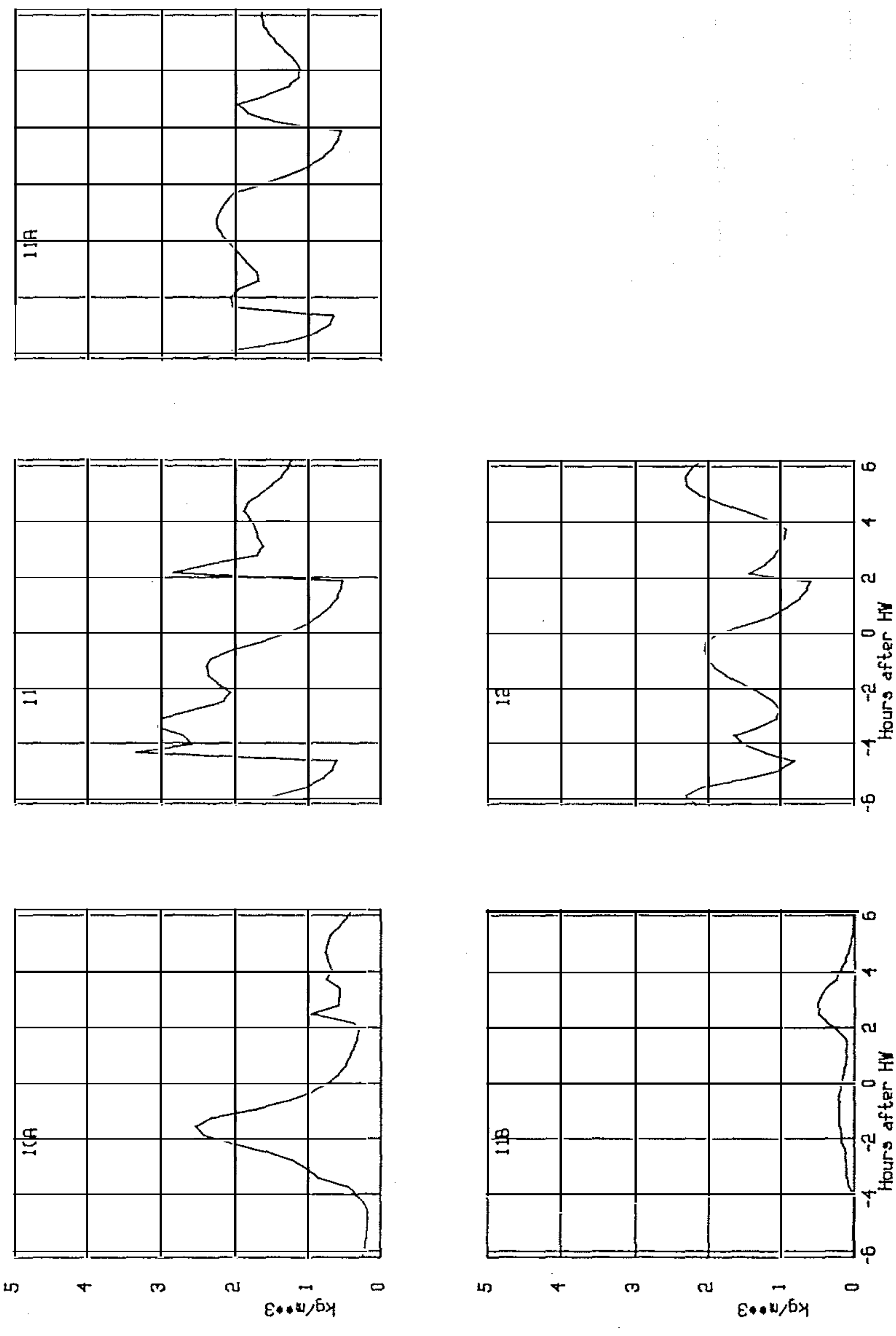

Fig 18 Simulated suspended mud concentration
after several neap tide.

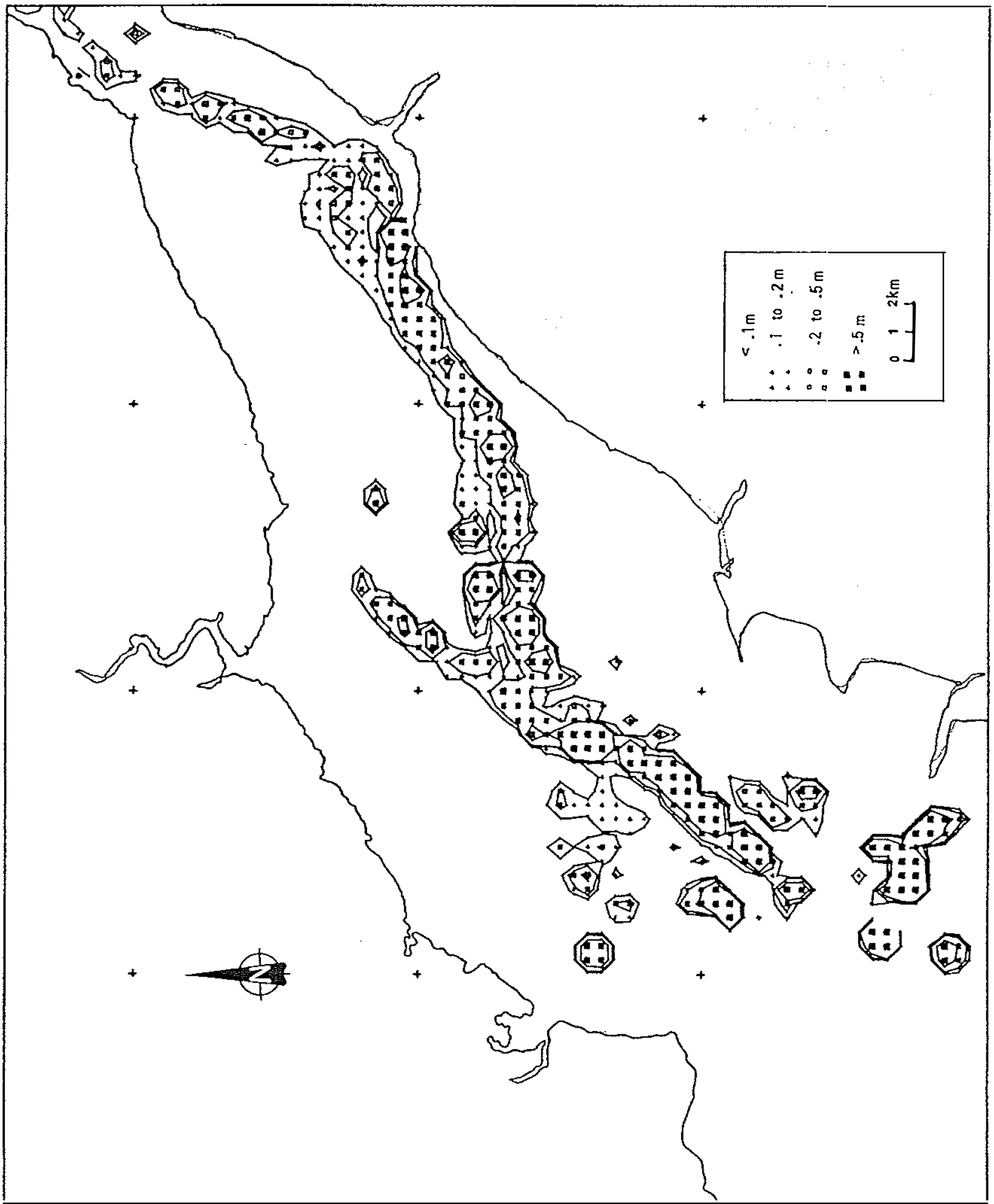

Fig 19 Simulated distribution and depth of fluid mud layer at HW slack neap tide

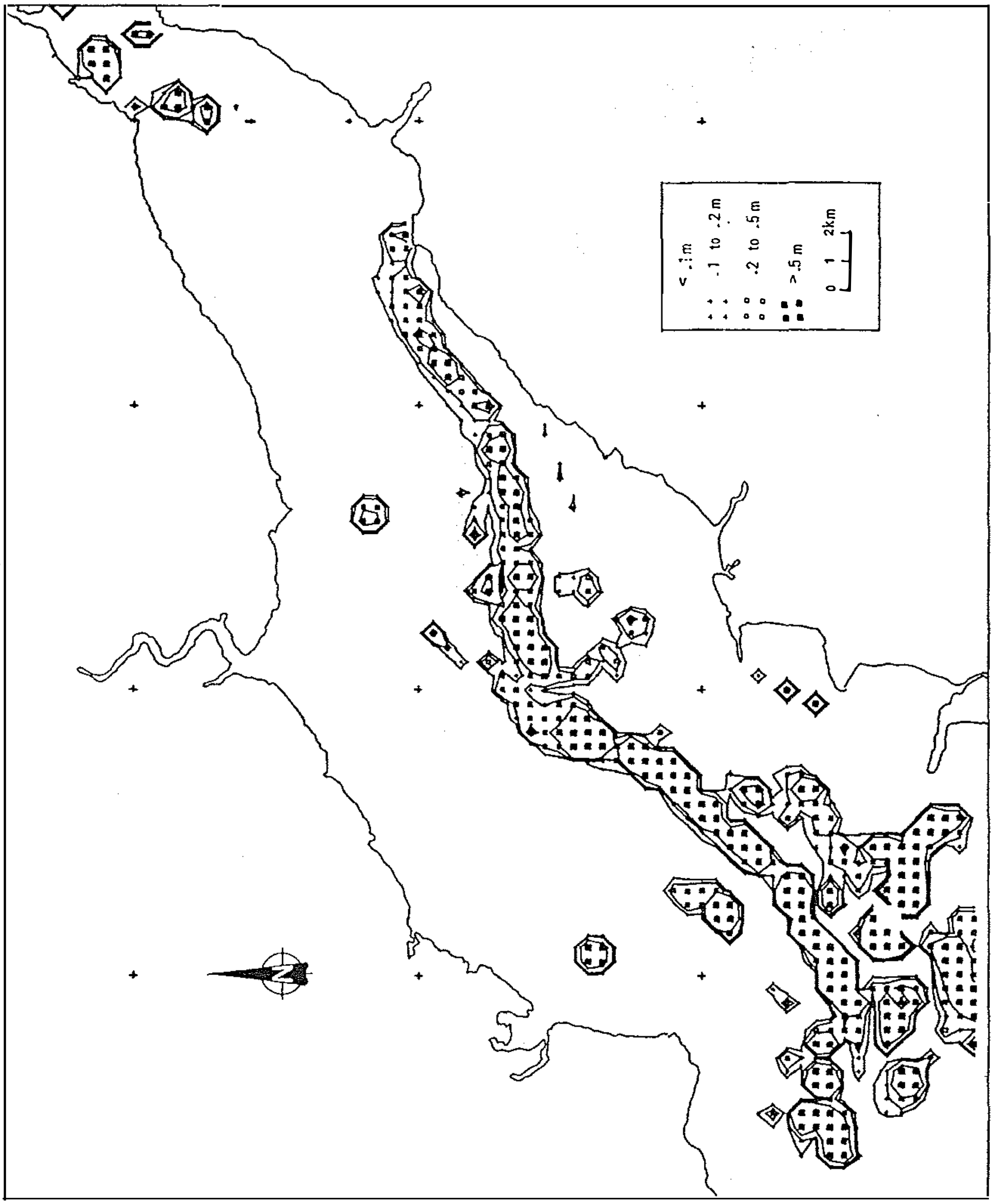

Fig 20 Simulated distribution and depth of fluid mud layer at LW slack neap tide

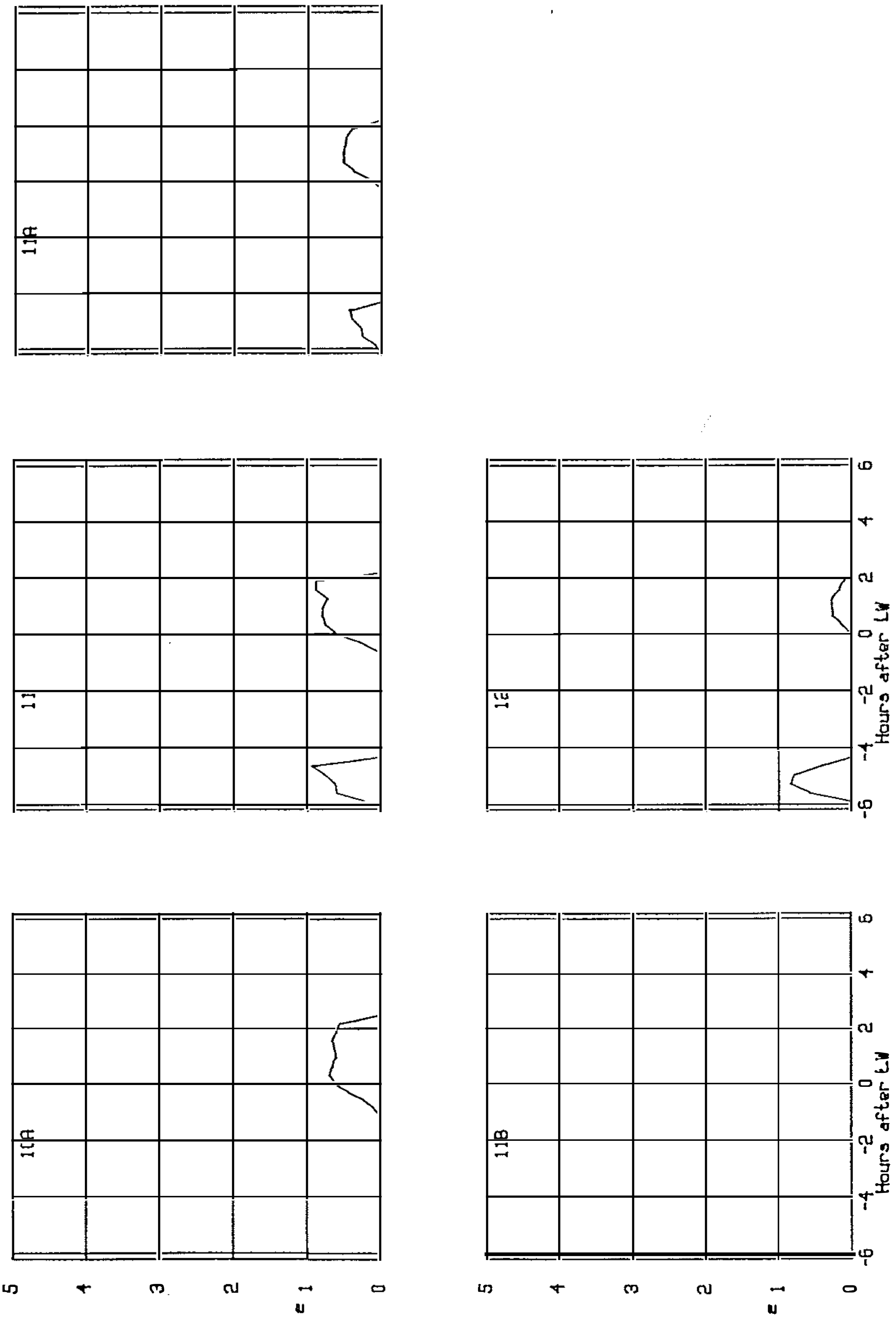

Fig 21 Simulated growth and entrainment of fluid mud layer at neap tide.

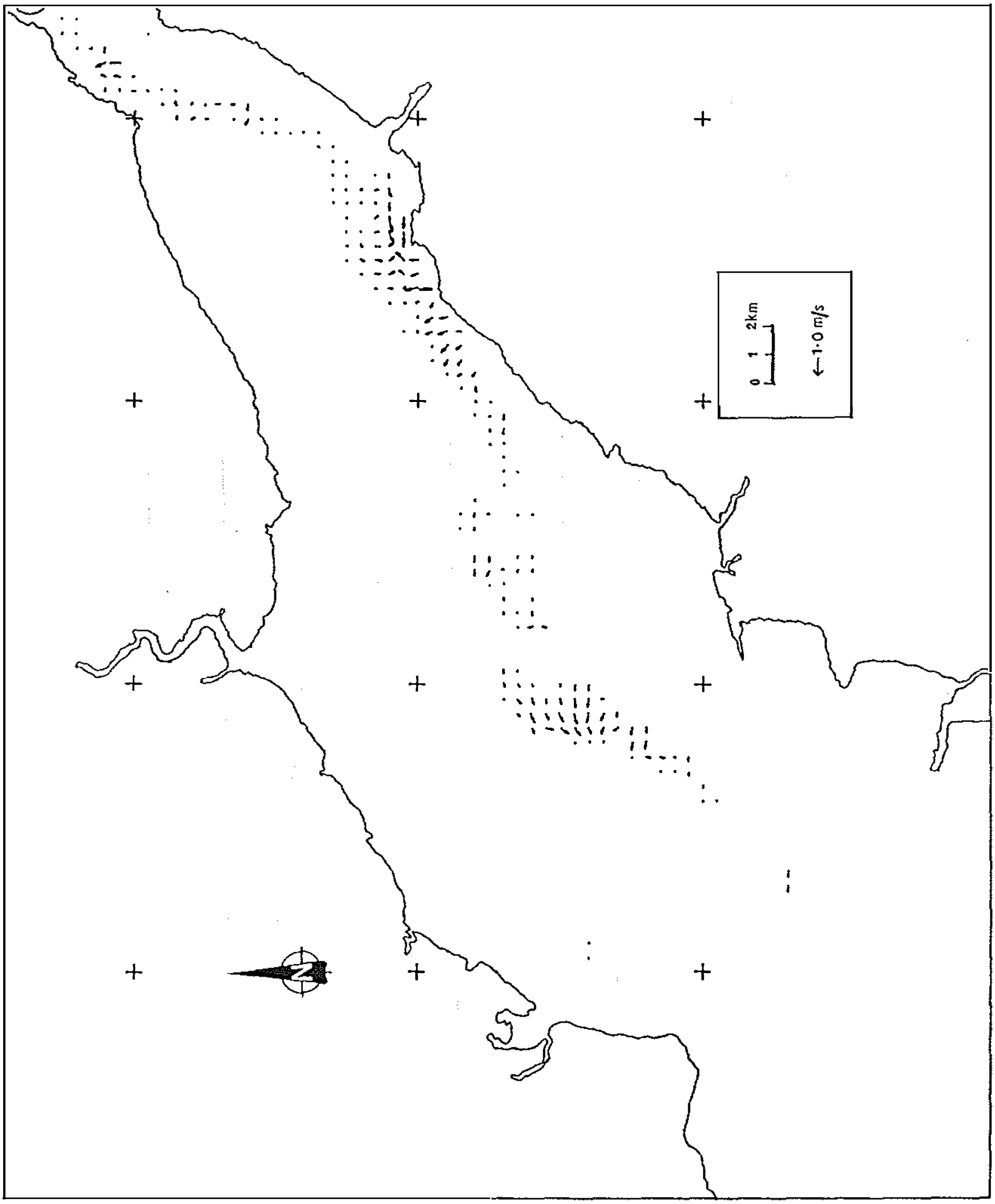

Fig 22 Simulated fluid mud velocity vectors at HW slack neap tide.

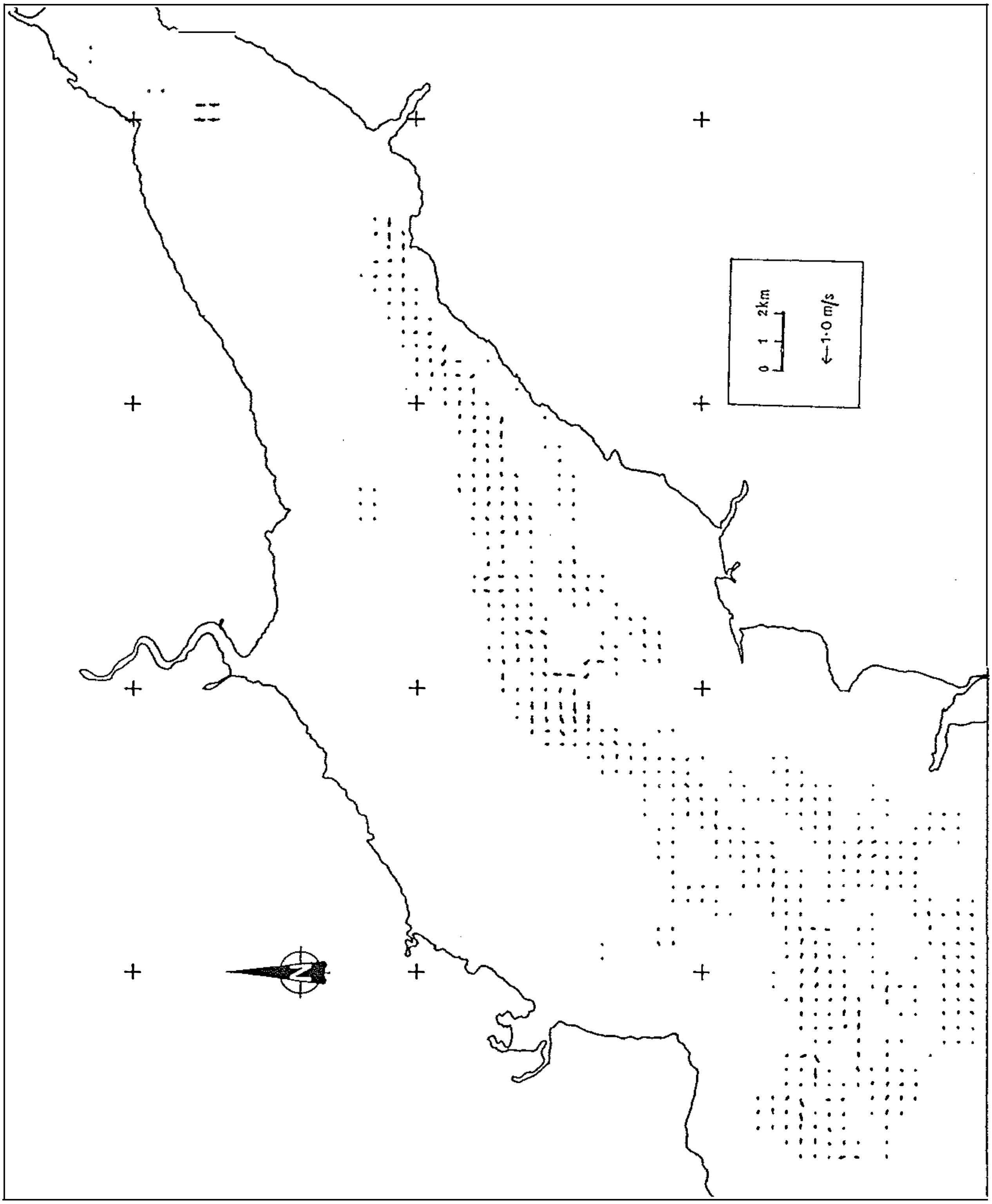

Fig 23 Simulated fluid mud velocity vectors at LW slack neap tides.

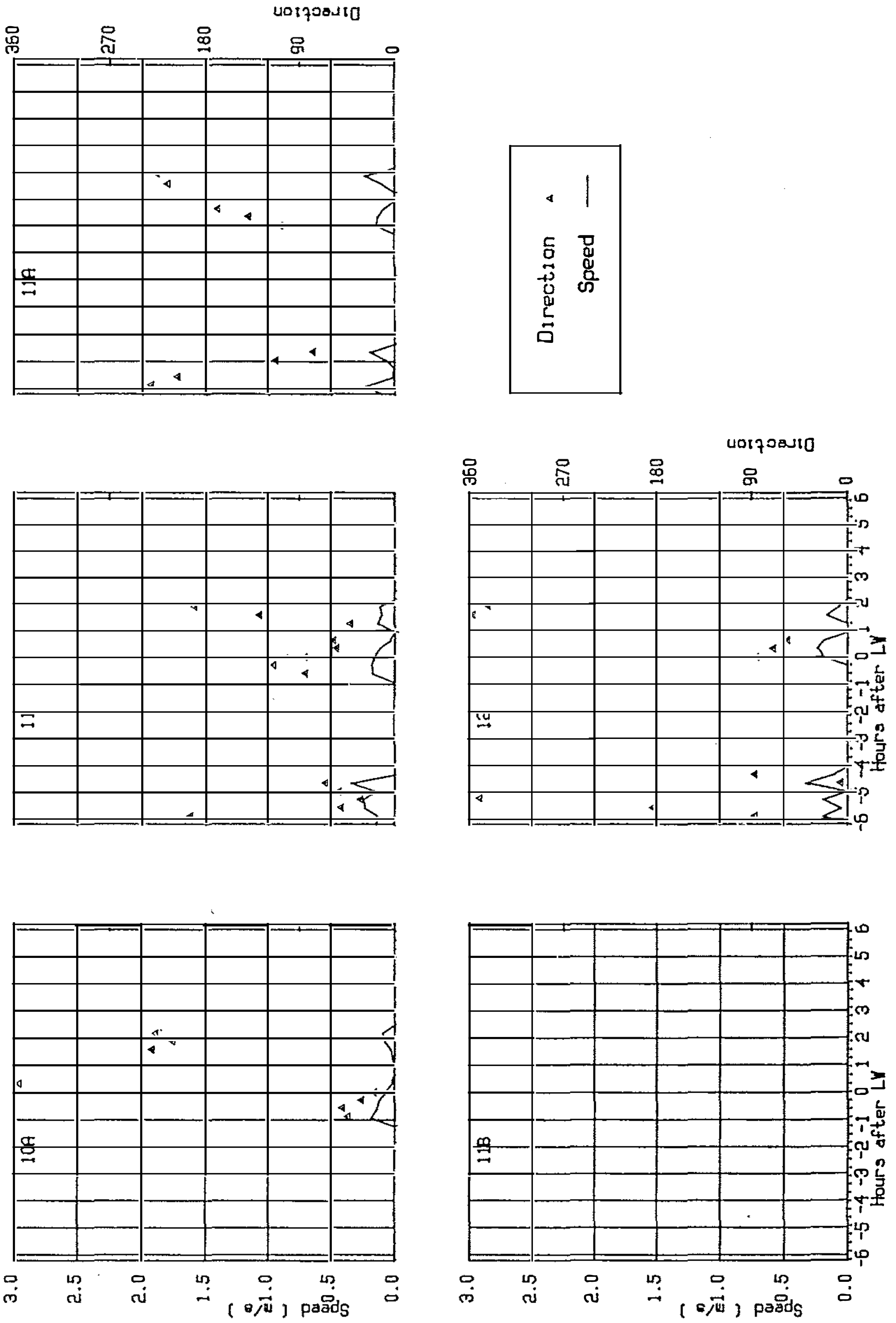

Fig 24 Fluid mud velocities Neap tide

APPENDIX C4

Field settling velocities of estuary muds

VII. FIELD SETTLING VELOCITIES OF ESTUARY MUDS

T. Neville Burt
Hydraulics Research Ltd.
Tidal Engineering Department
Wallingford, Oxfordshire OX108BA
United Kingdom

ABSTRACT

To improve the ability of numerical models to predict sedimentation of harbors and channels there is a pressing need for meaningful data and equations to describe the settling of fine cohesive sediments from suspension.

As a step in this direction this paper reviews the principles involved then goes on to describe a field study carried out in the Thames Estuary using the "Owen Tube", a settling column adapted for field use which has the advantage of not breaking up the natural flocs. Over 200 field measurements were made during 3 years and the data used to investigate the effects of concentration, particle size, salinity and tidal range.

A reasonable general equation is derived from Thames data showing that concentration completely dominates the process. Finally, the Thames data are compared with data from other estuaries, obtained in the context of project studies.

INTRODUCTION

The Need for Relevant Equations

In a typical year 10 million tons of fine sediment (as opposed to other materials) are dredged from Britain's ports, harbors and navigation channels. With present average dredging costs of about $4.00 per ton this amounts to an annual expenditure of $40 million. With the trend towards larger ships many ports have considered the economics of dredging and maintaining deeper channels. Many of those concerned with assessing the economics have asked for the advice of Hydraulics Research Limited or similar institutions around the world. How does the laboratory make a reliable prediction of sedimentation rates? Reliability is obviously important when such large sums of money are involved. An over-estimate may unreasonably rule out a proposed development. An under-estimate could lead to economic disaster.

It has never been possible to physically model the process of sedimentation because all the relevant parameters cannot be scaled at the same time. The advent of cheap and powerful computing and therefore of the numerical model has, however, begun to offer a solution since it depends not on scale relationships but on equations. The ability to model flow behavior has now reached an advanced state and the flow field and its time variation can be reliably predicted. However, when it comes to adding the sedimentation process, equations are often used which are at worst some guesswork and at best are based on laboratory tests which may have given inappropriate results. For example, Owen (17) showed that measurements in the field invariably gave higher settling velocities than are obtained by laboratory methods. It was this lack of definitive equations which stimulated the initiation of the research described in this paper. It appears that the main reasons why this has not been thoroughly studied previously are the difficulty of measuring the settlement of undisturbed suspension sediment in its natural environment and consequent high cost of obtaining a substantial data bank.

The author has been involved in a number of sedimentation studies where it has been necessary to determine the field settling velocity of the natural suspended sediment. This was done using the Owen tube and in each case it was found that quite large differences in settling velocity occurred. It was, therefore, decided to concentrate on one estuary, the Thames, to try to identify those factors which influenced the settling velocity and quantify their effect.

Before discussing this further it is appropriate now to consider the basic settling process and how it is affected by flocculation.

The Settling Process

The settling velocity of cohesionless particles, such as coarse silt, sand and gravel (using the BS size classification (2)) in a low concentration suspension can be calculated using well defined expressions (e.g. Stokes' Law) from the relative density, size and shape of the particles, since only the forces of gravity and flow resistance of the particles are involved. When the particle concentration is high and the various particles interact to alter the flow resistance the fall velocity diverges from the low-concentration value as a function of the volumetric concentration of the particles in suspension. Several of the formula describing this divergence are reviewed by Happel and Brenner (6).

The settling of cohesive particles, however, cannot yet be calculated from any theoretically derived expression. Such particles are usually in the fine silt and clay size ranges, where other motions are significant compared with gravitational motion. There is Brownian motion, local shear (due to local flow gradients) and differential settling. In general, inter-particle collision due to local shear is the most important mechanism in estuaries. Brownian motion becomes important only when concentrations exceed approximately 10 g/l.

Brownian motion could maintain the very small particles in suspension virtually indefinitely were it not for another mechanism. The small particles collide with each other as they move and cohesion causes them to adhere to each other and form aggregates of particles, or flocs. The flocs can be large enough to overcome Brownian motion and settle out. The size of a floc depends on the frequency of collision of particles and on the strength of the cohesive forces. The floc forms are complex functions of the particle mineralogy and the electro-chemical nature of the suspending medium.

Flocculation

As stated, flocculation depends on collision and cohesion. Both processes have been reported extensively by Krone (9), Einstein and Krone (4,5). As it is not the purpose of this study to try to re-define the settling process but rather to quantify it and investigate those factors which influence it in an estuary, only a brief review is included here.

Collision

The probability of collision of single particles due to Brownian motion is expressed by Leivich (11) as:

$$I = \frac{4\,k\,T\,n}{3\,\mu} \qquad (1)$$

where, I is the number of collisions per unit time, k is Boltzmann's constant, T is absolute temperature, n is number of particles per unit volume and μ is dynamic viscosity. In a typical British estuary the temperature varies by about 7% between summer and winter which has an indirect effect on collision frequency by strongly affecting viscosity. However, it is evident from Equation 1 that the concentration of material in suspension is likely to have the biggest single influence on the frequency of collisions bearing in mind that concentrations may vary between about 10 ppm and 100,000 ppm (e.g. Milford Haven and River Parrett respectively).

Cohesion

The mutual forces experienced by two or more clay particles in close proximity are the result of the relative strengths of the attractive and repulsive forces. These forces are discussed in detail by Lambe (10). The attractive forces are due to the interaction of the electrical fields formed by the dipoles in the individual molecules. The repulsive forces are due to ion clouds of like charge repelling each other. The result can be either attractive or repulsive depending on the relative magnitudes.

In suspensions with a very low ion concentration the ion double layer is large and the repulsive forces keep the particles too far apart for the attractive forces, which vary inversely with the seventh power of distance between particles, to come into effect. As the ion concentration is increased the double layer is reduced in size and the repulsive forces become small enough for particles to come close together and for attractive forces to prevail. The particles then join to form flocs.

Apart from the properties of the material the other factor affecting cohesion that can vary in an estuary is the salinity which is related to the ion concentration. With negatively charged clay minerals, such as montmorillonite or illite, in suspension the addition of sodium chloride causes flocculation to occur, the monovalent sodium cations forming the ion cloud around the clay particles. Sea water, in theory, has an even stronger effect because it usually contains several salts of higher valency metals.

From the above discussion it may seem that flocs may grow indefinitely in size. However, as the flocs get bigger they fall faster until the fluid shear exerted on them becomes greater than the interparticle bond strength. When the two forces are equal the flocs have reached a terminal size and settling velocity.

THE OWEN TUBE

The Owen tube was developed by Owen (17) in about 1969 to provide relevant settling velocity data for engineering applications. It is a field operated version of a laboratory settling tube and as such circumvents most of the arguments about the relevance of laboratory measurements. Settling tests are carried out using water at the same temperature, pH and salinity, the same suspended solids concentration and the same floc sizes and specific gravities as existed at the sampling point immediately prior to sampling.

Apparatus and Procedure

A full description of the apparatus is given in Ref. 17. It is illustrated in Fig. 1. Only a general description is necessary here to convey the principles involved. The Owen tube is essentialy a 1 m long perspex tube of 50 mm internal diameter. It is initially open at both ends and is lowered, usually from a boat, into the water where it is suspended horizontally in line with the flow at the depth where sample is desired. After a short time, when flow through the tube has been established the ends of the tube are closed off and the tube containing the sample is raised to the working deck. The tube is designed so that as it is lifted out of the water it automatically swings to the vertical position. At this precise time a stopwatch is started and the settling test has begun.

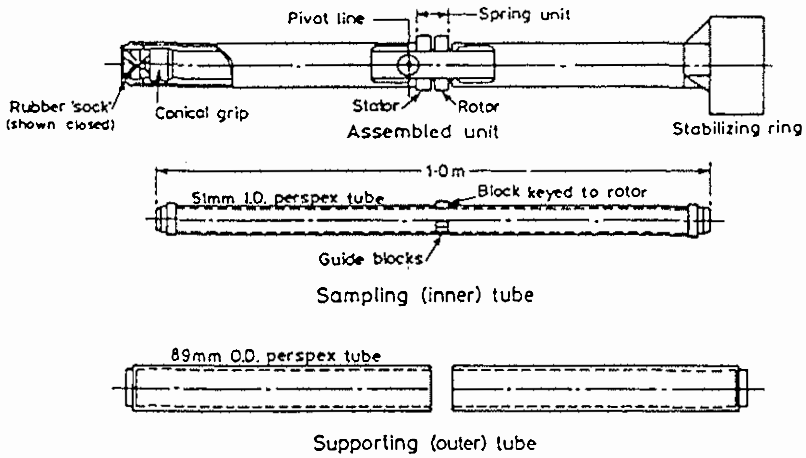

Fig. 1. Outline Drawing of Sampling Instrument

Once in a frame on deck, samples can be withdrawn from the bottom of the tube. Samples of approximately 250 ml are taken after 3, 6, 10, 15, 25, 40 and 60 minutes. The last sample taken empties the tube. The samples are labelled and returned to the laboratory where volumes of the suspensions and their suspended solids concentrations are measured gravimetrically.

Calculation of Results

The calculation of results is fully described in Ref. 17 with worked examples. An outline of the procedure is given here.

(i) The volume of the samples are added and checked against the known volume of the tube to ensure there has been no leakage.

(ii) The height of water in the tube after each sample has been removed is calculated from the cumulative volume of samples divided by the cross-sectional area of the tube. This also indicates the height through which the solids in each sample settled.

(iii) Cumulative dry weight for each sample is calculated and expressed as a percentage of the total weight of sediment.

(iv) The concentration of solids in the original tube is obtained by dividing the total weight of sediment by the total volume of water.

(v) The settling velocity grading curve is then obtained by a graphical method which essentially evaluates the percentage of flocs in the suspension which have a settling velocity less than that defined by a specified time, from a semilog plot of cumulative percentage weight against time.

(vi) Finally, if desired, the settling velocities can be adjusted to compensate for temperature effects on viscosity using tabulated values.

Although somewhat involved this is a standard and reliable method of determining particle (or rather floc) fall velocity distribution. It is known as the bottom withdrawal method.

Form of the Results

The end product of the above precedure is a semilog plot of settling velocity vs. percentage by weight of solids having a settling velocity less than the plotted value.

A typical plot is shown in Fig. 2. It resembles a particle size distribution familiar to soils engineers and, in the case of cohesionless material is qualitatively the same thing. For cohesive materials it is definitely not the same thing because neither the shape nor the specific gravity of the flocs is constant and the concept of an equivalent Stokes diameter becomes meaningless. For instance, a floc having a settling velocity of 1 mm/s would indicate a Stokes diameter of 0.04 mm when it could have a physical size of more than 1 mm. No attempt is made in this study to infer a size from the settling velocity data except where material has been deliberately de-flocculated for that purpose (see later section on effect of particle size).

The settling velocity distribution graph is the starting point for examining the influence of various parameters on the settling velocity of Thames mud.

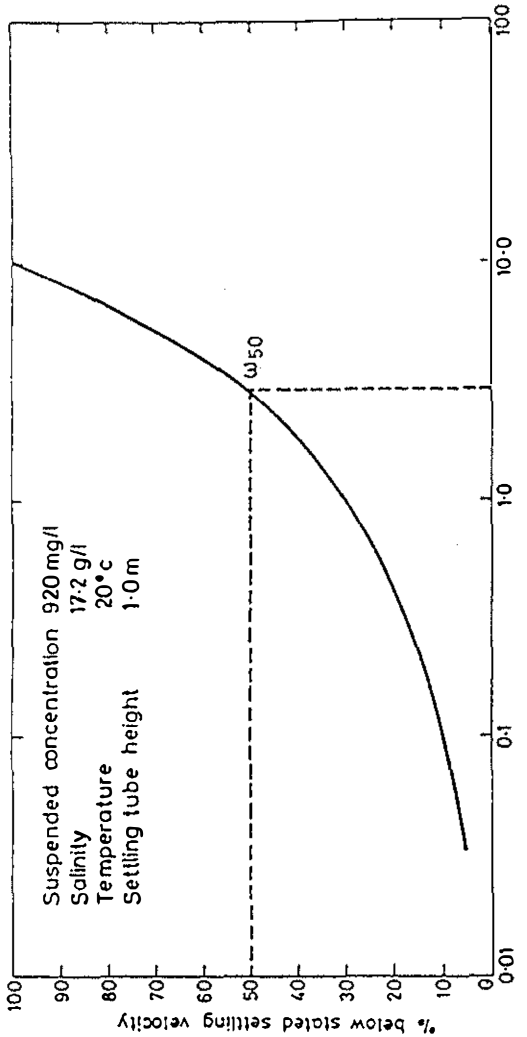

Fig. 2. Typical Settling Velocity Distribution

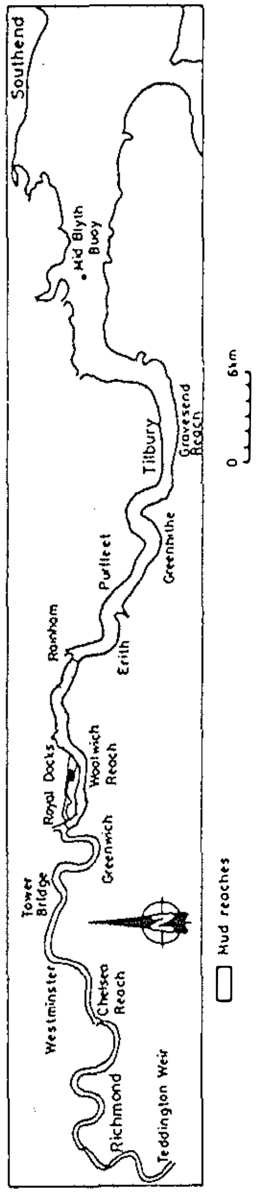

Fig. 3. The Thames Estuary

MEASUREMENTS IN THE THAMES ESTUARY

There were several reasons why the River Thames was chosen for this study.

(i) A good knowledge of the estuary already existed, in particular the author had studied the sediment transport regime (8,18).

(ii) A good range of suspended solids concentration exists (i.e. up to about 3,000 ppm under normal circumstances).

(iii) A good range of salinities exists (i.e. 1 to 32 ppt in the 'mud reaches' (Fig. 3) without the complication of stratification).

(iv) The estuary was reasonably close to the laboratory.

(v) The results would be of specific interest in the context of a number of present studies.

(vi) Some of the earliest measurements with the Owen tube had been made in the Thames thus enabling a comparison to be made of settling characteristics a decade apart.

Field Measurements

Data were collected with the Owen Tube during three separate periods, in October 1981, September 1982 and November 1983. Obviously in a field study of this type it is not possible to exercise any control over conditions but by careful selection of survey dates, tidal times and positions and making full use of existing knowledge (8,18) it was found possible to obtain a good range of salinities and suspended solids concentrations.

The first measurement in 1981, established a fairly good data base but there were some gaps noteably at the extremes of low and high salinity. The second measurement was designed to fill those gaps but it was found impossible to obtain high concentrations of suspended solids at the extremes, perhaps not surprisingly because, almost by definition, they occur rarely at the turbidity maximum. The first analysis of the results of the first two measurements is presented in Ref. 3.

The third measurement was designed primarily to study the indirect effects of tidal range, i.e. flow velocity and associated turbulence, by regular sampling for seven days from spring to neap tides.

Two tests were carried out in 1969 specifically to investigate the effect of particle settling velocities of the then new Woolwich Ferry Terminals. Samples were taken near the northern terminal during two periods of spring and neap tides. Full details of this work are reported in Refs. 7 and 15. The other 1969 data were from eight samples taken at Tilbury.

The conditions, range of values, number of samples obtained, etc., are shown in Table 1. Also shown in the table are, as far as is known, the same information for the earlier Thames measurements.

Table 1 - Summary of Thames Measurements

Date	Location	Concentration Range ppm	Tidal Range	Salinity ppt	Temp °C	No of Samples
Aug 69	Woolwich	300-2630	Spring	7	20	14
Sept 69	Woolwich	54-256	Neap	7	20	11
Sept 69	Tilbury	101-344	Spring	24	19	8
June 71	Woolwich	52-449	Spring	1	16	7
Oct 81	Various	97-4720	Spring	Various	11	65
Sept 82	Various	130-2941	Neap	Various	19	34
Nov 83	Various	159-4841	All	Mainly mid-range	13	104

Processing of Results

As explained earlier the laboratory analysis of the Owen Tube samples produces a graph of settling velocity against percentage of material having a lesser settling velocity for each tube sample (Fig. 2). To simplify correlations with other parameters each graph is assumed to be reasonably well characterized by the value of W_{50}. The parameter W_{50} is the median fall velocity, being the fall velocity below which 50% by weight of the sample settled out. Comparative checks for the analyses were made with W_{30} and W_{70} values and comments are made on differences where appropriate.

Effect of Concentration

The introduction described the flocculation process and its effect on settling velocity and how the work of Leivich (11) indicated that concentration was likely to have the biggest single influence on flocculation. It is, therefore, not surprising that even a cursory examination of the Thames data reveals that concentration indeed dominates the settling behavior of suspended Thames mud. This effect must be described before it is possible to attempt any other correlation. Figure 4(a), (b) and (c) shows the relationship between median settling velocity, W_{50}, and concentration of suspended solids for the 1981, 1982 and 1983 measurement results. The log - log plots show quite a lot of scatter, indicating either random error or the existence of other influencing parameters, but nonetheless indicate a reasonable relationship of the form:

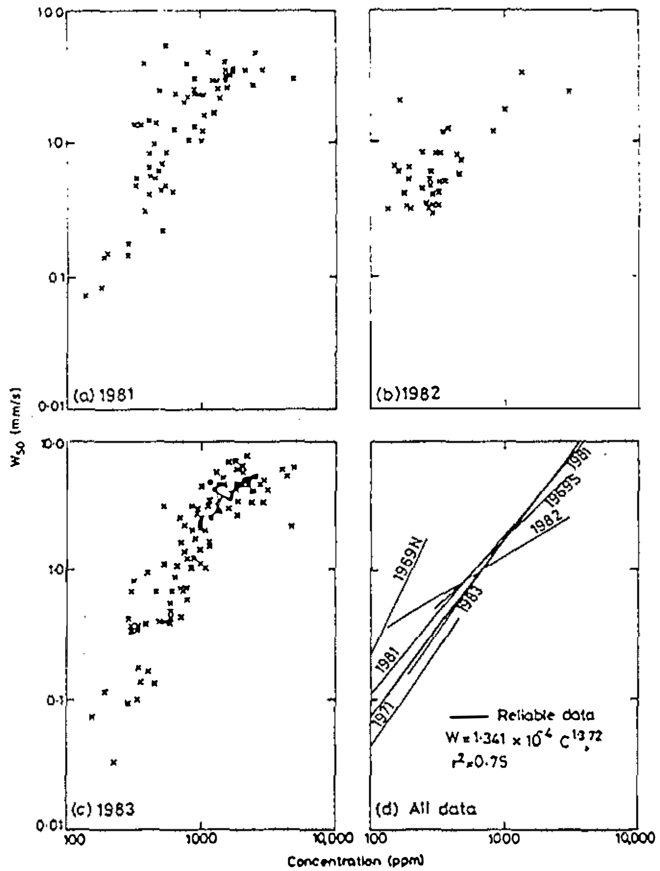

Fig. 4. Effect of Concentration on Median Settling Velocity

$W_{50} = C^{i}$

where i is termed the settling index. Figure 4 also shows that there is some similarity between the 1981 and 1983 results but a definite displacement of the 1982 data which had higher settling velocities for a given concentration.

It is interesting to compare these results with the earlier 1969 and 1971 results. The best fit lines are shown in Fig. 4(d) with the exception of the 1969 Tilbury data which showed no correlation with concentration. The lengths of the lines truly represent the range of concentrations covered.

Apart from the 1969 Woolwich neap tide data and the 1982 survey data the remaining data fit reasonably well together, but before simply rejecting them the circumstances were examined to see if there was anything exceptional or common to both which may give a clue to significant influencing parameters. Turbulence as indicated by tidal range, temperature and salinity were all ruled out on the grounds that there was nothing exceptional about their values. The only clue found was that the de-floceulated particle size analyses showed that the median size of the 1982 suspended material was only half that of the 1981 material. This is further discussed in a later section (section, effect of particle size).

Rejecting now the two uncharacteristic data sets, the remaining data was processed as a single set. The best fit equation was:

$$W_{50} = 1.341 \times 10^{-4} \, C^{1.37} \qquad (3)$$

where the units of C are mg/l and W_{50} are mm/s.

This equation with a correlation index (r^2) of 0.75 could be used with some confidence for predicting median settling velocity in the Thames (or more precisely, in a quiescent Thames, but the problems of deposition from flowing water will be left for future consideration) knowing only the concentration.

It is interesting to compare this empirical value of 1.37 for the settling index with that obtained by Krone (9) theoretically from consideration of collision probability. This approach leads to a prediction of the number of particles present in a floc after a finite time and hence relative floc size and hence a relative settling velocity. This method predicts that settling velocity should be proportional to the concentration to the power 1.33.

It needs to be stressed that the derived equation for W_{50} is only applicable

[illegible] begins to take place. That is when there is a sufficient volumetric flux of sediment downwards to induce a significant volumetric flux of water upwards thus reducing the settling velocity with increasing concentration.

Having established the basic concentration effect we can now move on to see if the equation should be refined to take account of other parameters.

Effect of Particle Size

Before discussing its possible effects it is necessary to attempt a definition of what is meant by particle size. Since the settling process is governed by flocculation and flocculation depends on forces existing at molecular levels it becomes difficult to say even what is meant by a particle. Once again, therefore, particle size has to be defined by the way it is measured. The technique used was a standard settling test performed by the HR Sedimentation laboratory using deflocculated samples. The result is a Stokes equivalent diameter which may or may not have some physical significance but at least gives a consistent basis for comparison between samples.

Only the 1981 and 1982 samples were analyzed in this way. The first stage was to group all the data together and test the following hypotheses:

(i) High concentration samples implicitly contain a greater proportion of large particles than low concentration samples. This would contribute to higher concentration samples having a higher median fall velocity.

(ii) For samples of equal concentration, differences in particle size will give rise to differences in median fall velocity.

A plot of concentration vs. D_{50} (not illustrated) appeared to disprove the first hypothesis. Furthermore, for samples of equal D_{50} (about 2.3 micron) the normal concentration dependence of W_{50} was found. This is illustrated in Fig. 5(a). Figure 5(b) tests the converse by plotting the settling velocities vs. D_{50} of samples having the same concentration, about 350 ppm. At this concentration no correlation was found.

When the 1981 and 1982 data were grouped separately the average median particle size for 1981 was 0.0063 mm and for 1982, 0.0031 mm, half the size. For equal concentrations of 200 ppm the 1982 value of W_{50} is about double the 1981 value. This could be explained on the basis that smaller particles have a greater tendency to

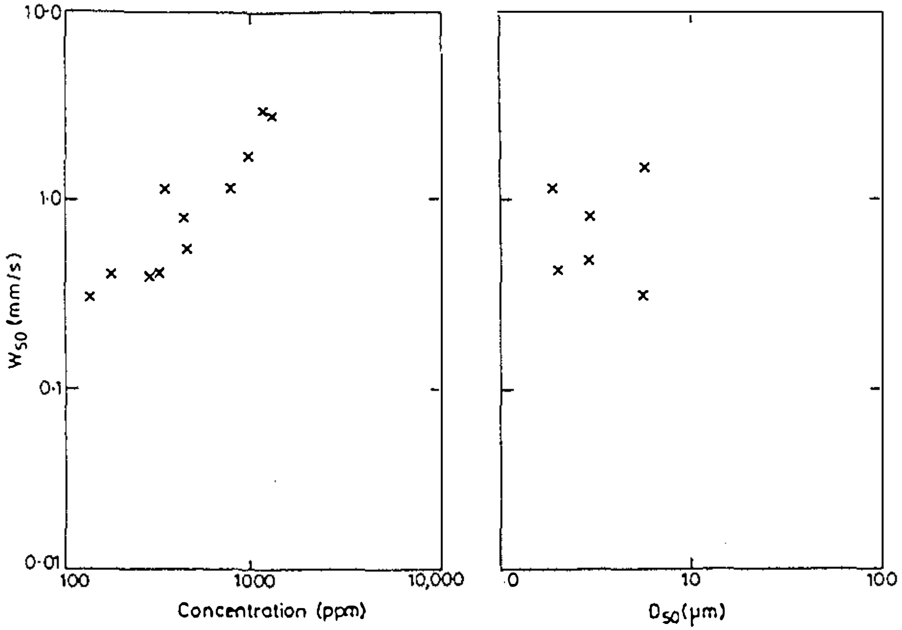

(a) Samples of similar D_{50} (b) Samples of similar concentration

Fig. 5. Effect of Particle Size on Median Settling Velocity

to reverse for concentrations greater than 500 ppm, but there were few samples in this band in 1982 and no great weight should be attached to the evidence.

Taken as a whole it is not possible to do more than suggest that median fall velocity can be affected by variations in the median deflocculated particle size. A corollary conclusion is that the material found in suspension in the Thames estuary is quite consistent in its particle size distribution most of the time.

Effect of Salinity

It was suggested in the introduction that salinity could affect the strength of the cohesive bond between particles and in particular that common salt aided the flocculation of negatively charged clay minerals. This charge is the result of isomorphous substitution, broken edges from abrasion during the weathering process in the source areas (13), or the hydrogen of exposed hydroxyls replaced by an exchangeable cation. Because of this it seems probable that there is considerable variability in the strength of the charge so a uniformity of the effect of salinity would not be expected from one estuary to another.

Owen's work on Avonmouth mud in the laboratory confirmed the flocculating effect of salinity (14). His results are summarized in Fig. 6 showing a very nearly linear effect of salinity varying between 0 and 28 ppt on fall velocity. Results shown by Krone (9) and Allersma et al (1) are also replotted in Fig. 6. Krone found that for suspended solids concentrations up to 530 ppm the settling velocity of a cohesive sediment was independent of salinity above 5 ppt. Allersma's results show that, for example, at a salinity of 5 ppt the settling velocity increased to 30 times its fresh water value but at 25 ppt the settling velocity was only about twice its value at 5 ppt. Migniot (12) too observed that settling velocity was constant at salinities above 3 ppt for low suspended solids concentrations and above 10 ppt for high concentrations (an effect also evident in Krone's results).

This weight of evidence led to the expectation that salinity would play a significant part in determining the settling velocity of the Thames suspensions. The results, plotted in the same form as in Fig. 6, are shown in Fig. 7 using the 1981 survey data which covered the range of typical salinities and concentrations experienced in the Thames. Figure 7 clearly shows that varying salinity has no observable effect on settling velocities measured 'in situ' for any concentration in the range measured. This is contrary to expectations and some explanation must be sought.

The most likely explanation, in the author's view, lies in the difference between laboratory and field measurements. The results shown in Fig. 6 are all based on laboratory work where samples, either reconstituted or in natural water (as with Allerama) had to be resuspended by mechanical agitation. Flocculation is a time-dependent phenomenon and it is therefore suggested that both the time taken for settling through laboratory columns and the associated settling velocity gradient do not allow full re-flocculation to take place. A clue that this is so is given by comparing the absolute values of W_{50} obtained by Krone, Owen, etc., with those obtained from the field measurements. The latter are at least one order of magnitude higher.

The implication is that in the Thames estuary, if not in all muddy estuaries, material is held in suspension long enough for a much greater degree of flocculation to occur not only at high salinities but also for the same degree of flocculation to occur at low salinities. In other words within the accuracy of measurement salinity does not affect the ultimate median floc size although it affects the speed with which the flocs form.

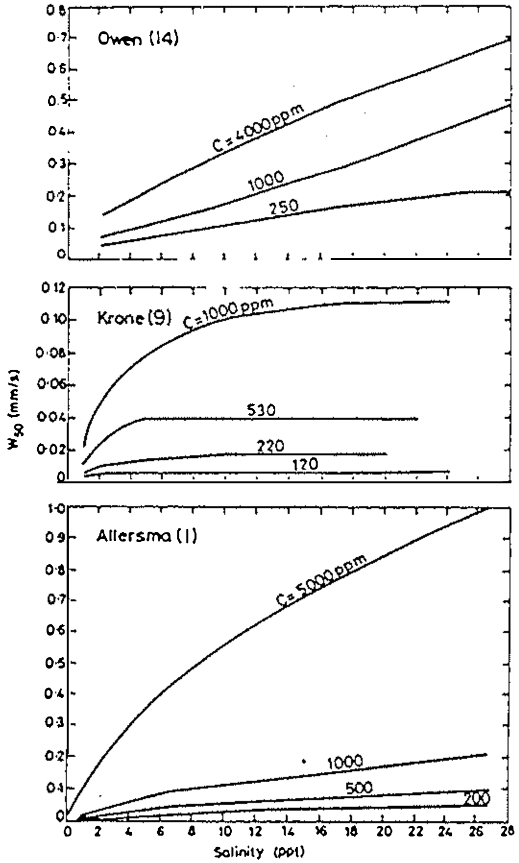

Fig. 6. Effect of Salinity on Settling Velocity: Previous Studies

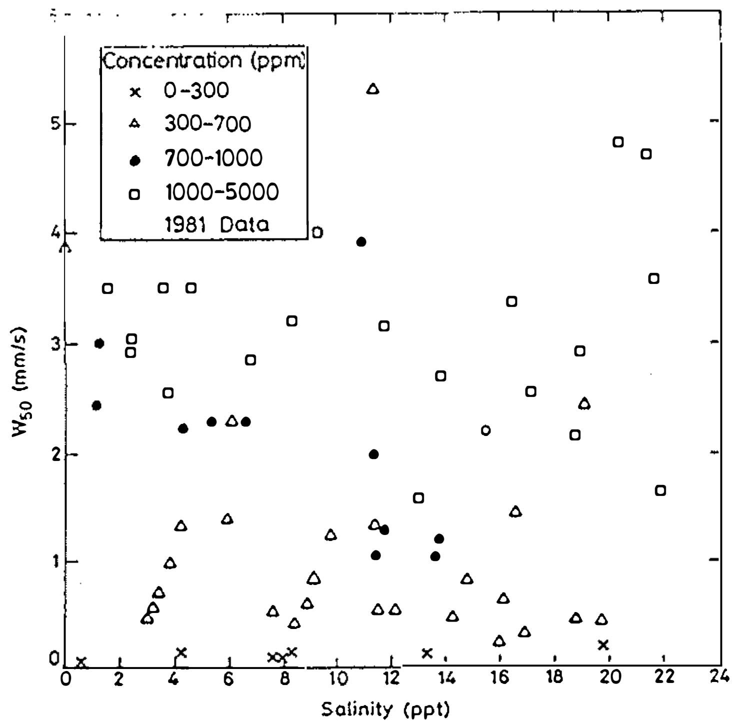

Fig. 7. Effect of Salinity on Settling Velocity: Thames Field Studies

Effect of Tidal Range/Turbulence

Owen (7) noted that the 'random movement of the water associated with turbulence brings fine sediment particles into frequent collision with each other and they flocculate provided that the fluctuating internal shear generated by the turbulence is not greater than the bond strength between the particles. It can thus be seen that the degree of turbulence can have widely differing effects'. It is suggested in other words that increasing turbulence may enhance flocculation and at the same time limit the size of flocs that can be sustained.

Owen went on to investigate the effects of turbulence using the data obtained from Woolwich in the Thames in 1969 (15). He observed that 'during the spring tide the settling velocity increased approximately linearly with suspended solids concentration. During the neap tide the settling velocity was found to increase approximately with the square of suspended concentration'. (It is interesting to reflect here that in an earlier section the settling index for all the accepted data was 1.37.) The neap tide settling velocities were consistently higher than the spring tide values and also showed a stronger dependence on concentration. Both these facts lead to the implication that the higher turbulent energies associated with spring tides have a more disrupting effect on the flocs than a constructive one by inducing more collisions.

Turning now to the Thames data as a whole, it can be divided into groups described as spring tide data and neap tide data with the dividing line set at mean tide. Figure 4 has been replotted on this basis in Fig. 8, dividing also the 1983 data which covered a cycle from springs to neaps. The neap tide data is shown as dotted lines in the figure. The 1983 data was designed specifically to examine tidal range effect so this data alone is shown in Fig. 9 where W_{50} is plotted against tidal range for a number of concentration bands. Despite the large scatter it is clear from these figures that no correlation exists for any concentration band. It is evident that the conclusions drawn from the 1969 data are contradicted by the 1983 data in terms of absolute settling velocities for any specified concentration, although a settling index is higher in both cases than for any of the spring tide data, but this too is contradicted by the 1982 data which showed a lower concentration dependence than any other of the data.

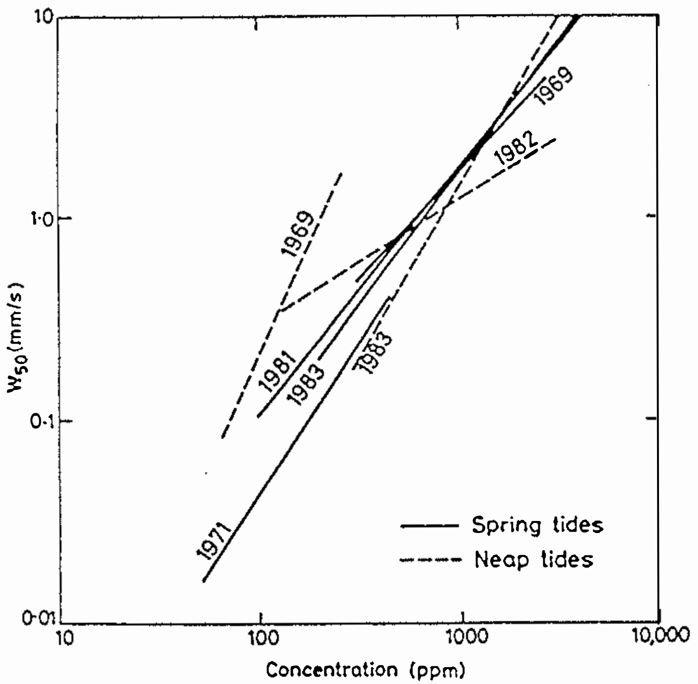

Fig. 8 Effect of Tidal Range: Springs and Neaps, all Data

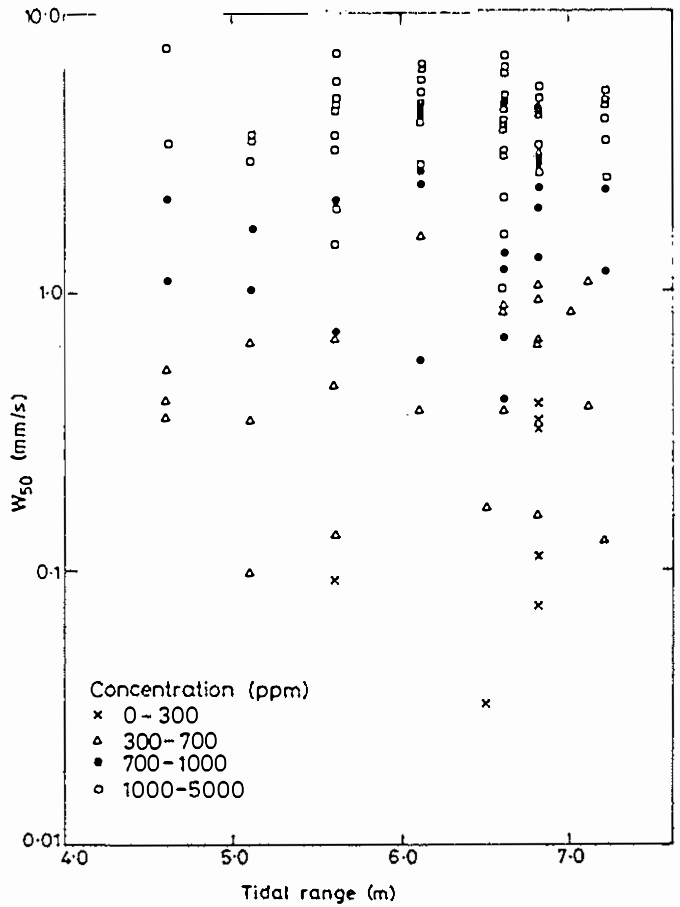

Fig. 9. Effect of Tidal Range: all Ranges, 1983 Data

It must be concluded on the above evidence that tidal range has no consistent effect on settling velocities. This is not to say that turbulence has no effect but rather that variations in tidal range do not induce relevant changes in turbulence. Relevant turbulence is likely to be that which is of a scale comparable with the size of the flocs.

Effect of Settling Height

This has been included for the sake of completeness rather than to add any new evidence. Variations in the settling velocity through the water column possibly occur in the Thames but were not studied. Owen (14) studied the relevance of settling height by using laboratory columns of different lengths and concluded that a minimum height of 2 m was required to achieve maximum settling velocity. However, in view of comments made in the earlier section on salinity it seems likely that in these tests flocculation was not fully developed and differences due to settling height could equally be explained as the time required to achieve a certain degree of flocculation.

It follows that if flocs are fully developed in the field the settling height is irrelevant.

Effect of Temperature

As an extension to his earlier work on Avonmouth mud Owen conducted more tests to determine the effect of temperature (16). He concluded that the effect of temperature on the settling velocities of flocs formed in suspensions of varying salinity and concentration is largely limited to the effect temperature has on viscosity. After correcting for this there was a slight tendency to increase flocculation at higher temperatures and consequent higher W_{50}. Over the normal range of temperatures experienced in the Thames the effect was small in comparison to the effect of concentration or salinity.

Nothing in the field data contradicts this general conclusion. Referring again to Fig. 4 and the data in Table 1 it is evident that while the 1969 neap and 1982 data were obtained during warmer than average conditions when there was some evidence of higher settling velocities the 1971 Woolwich data was also taken during a warm (but not quite so warm) period and exhibited the lowest settling velocities.

A General Equation for the Thames

Attention has been concentrated on median settling velocity so far. Analysis of the type described was also carried out for values of W_{30} and W_{70}. The results did not contradict any of the conclusions drawn. Nevertheless for sedimentation predictions it is useful to try to encompass all the data in one equation. This was done using the method below.

Figure 4 showed plots of W_{50} vs. concentration. Similar graphs of W_{10}, W_{20}, etc., to W_{90} were produced using all the accepted data. The result was a series of displaced but parallel lines. Thus, it was seen that $W_n \propto C^i$ where i, the settling index, is constant for all values of n. The vertical displacement is expressed in the equation by the effect of another variable k:

thus, $W_n = kc^i$ (4)

and k is a function of n.

The values of k for each value of n were obtained from the data and the result is shown in Fig. 10. The general equation for the field settling velocity of Thames mud is thus:

$$W_n = C^{1.37} \times F(n) \quad (5)$$

where F(n) is $1.88 \times 10^{-4}\ n^{2.34}$, W is mm/s, C is g/l, n is %.

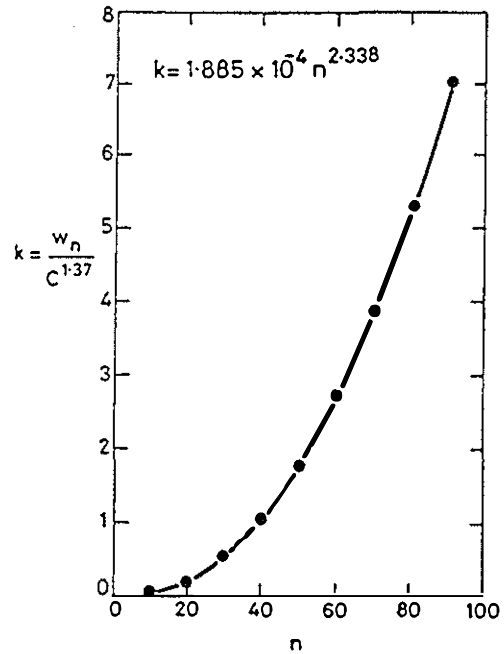

Fig. 10. General Equation for Thames Data

COMPARISON WITH OTHER ESTUARIES

A number of studies carried out by Hydraulics Research in recent years have included field measurements of settling velocity using the Owen tube. Results are available from Brisbane, Grangemouth, River Parrett and River Scheldt. Further information concerning these data is given in Table 2.

Table 2

	Brisbane	Grangemouth	Parrett	Scheldt	Thames
Location	Australia	Scotland	England	Belgium	England
Concentration range (ppm)	28-579	66-4049	420-10800	205-3285	50-5000
Tidal range		Spring	All (spring & neap)	Spring	All (spring & neap)
Salinity (ppt)	30				0-30
Temp (°C)					13-20
No. of samples	24	16	10	15	200+
D_{50} (microns)	4	20		20	4
% clay (by size)	40	28		22	32
% silt	42	66		58	67
% sand	18	6		20	1
% montmorillonite	30	0		20	15
% kaolinite	15	17		10	10
% illite/mica	5	17		10	25
% chlorite	0	17		0	20
% organics, etc	0	10		5	13
% non-clay minerals	50	39		55	17

The results are summarized in Fig. 11, together with the best-fit Thames data. There do not appear to be any consistent trends with these data. For example, Scheldt and Grangemouth muds have similar values of median particle size (D_{50} = 0.02 mm) as have Thames and Brisbane (D_{50} = 0.004 mm), but these similarities are not reflected in either the shape or position of the relevant lines in Fig. 11.

If total clay mineral content is important in determining potential flocculation then Thames mud with a total clay mineral content of 70% would be expected to show both the highest dependence on salinity and the highest settling velocities of all the muds. In fact it showed no dependence on salinity and only average settling velocities. The fact that Brisbane and Grangemouth muds with 50% clay minerals are closely related in Fig. 5 and Scheldt mud, with 40%, falls a little below is rather slender evidence on which to draw any conclusion.

Perhaps the most interesting conclusions to be drawn from Fig. 11 are that the slopes of the lines, the settling indices, are all contained within a band of 0.7-1.4, and that for a specified concentration, variations in W_{50} between estuaries

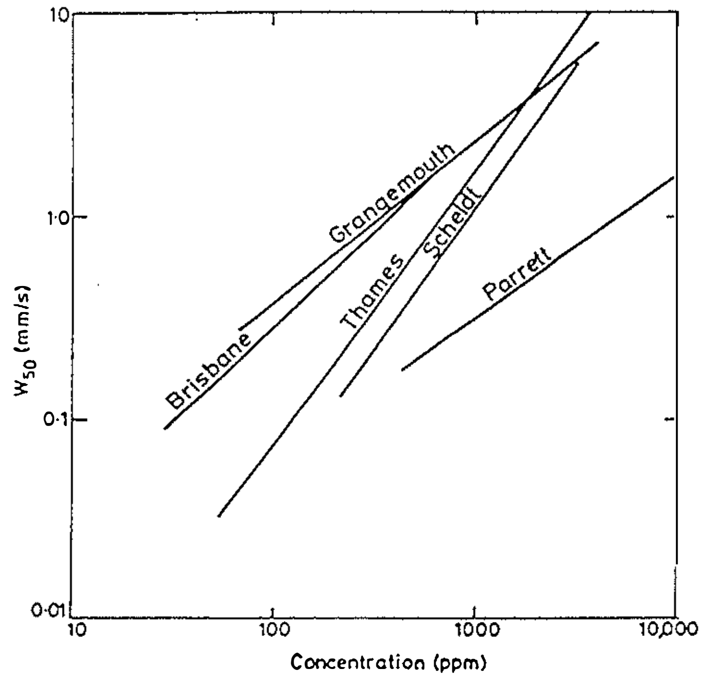

Fig. 11. Comparison of Data from Five Estuaries

can be up to an order of magnitude. It is also interesting to observe that if the Parrett data is ignored (not that there are any particular grounds for doing so), all the other data tend to converge when the concentration is in the region of 2000 ppm. This was also evident with much of the Thames data in Fig. 1(d). This may be a hint that at this sort of concentration the other influencing parameters are completely dominated by the concentration effect alone.

Finally, it should be pointed out that the Thames data are based on over 200 samples spanning several years, whereas most other lines in Fig. 11 are based on about 20 samples or less taken during one observation period.

SUMMARY AND CONCLUSIONS

1. There is a pressing need for meaningful equations describing the settling velocity of fine, cohesive sediments in order to advance the science of predicting sedimentation.

2. The large flocs fall faster although large flocs tend to have lower specific gravity so the effect is not simple.
3. Floc size is limited because as they get bigger and fall faster the fluid drag increases and the floc breaks up. Thus, at least in concept, there exists a terminal size and a terminal settling velocity.
4. Three sets of measurements were observed in the Thames Estuary covering a good range of salinities, concentrations and tidal ranges. Use was also made of earlier results from the Thames. Settling velocities were determined by the bottom withdrawal method and shown as settling velocity distributions for each tube.
5. The median settling velocity, W_{50}, characterizes the results sufficiently well to be used for studying correlations with relevant parameters.
6. The Thames field data conformed to the expected domination of the effect of concentration on W_{50}. The best fit line for the range of concentrations measured (up to 4000 ppm) was:

$$W_{50} = 1.34 \times 10^{-4} C^{1.37}$$

7. The power of C (settling index) of 1.37 is close to the 4/3 predicted by Krone from collision probability theory.
8. High concentrations in the Thames do not implicitly contain a greater proportion of larger (or smaller) particles than low concentrations: i.e. the size distribution is independent of concentration.
9. There is some evidence to suggest that smaller particles give higher settling velocities for concentrations up to about 1000 ppm. It is suggested that this could be due to greater flocculation.
10. Particle size distribution of suspended Thames sediment is quite consistent.
11. Contrary to expectations salinity appeared to have no effect on settling velocities. It is surmised that this is because, in the field, floes have time to develop to their optimum size whereas in the laboratory the effect of high salinity in speeding up flocculation is significant in the context of the settling time.
12. Field settling velocities are at least one order of magnitude bigger than lab values again pointing to the existence of larger flocs in the field.
13. Previous suggestions by Owen that variations in turbulence induced by variations in tidal range affected floc size and therefore settling velocities were not substantiated by the more intensive recent results.
14. Settling height is thought to be not significant in the field although it is in the laboratory because of the time taken for flocculation to occur in the laboratory.

15. There was no evidence of a significant temperature effect on settling velocity in the field data (after adjusting values for the effect on viscosity).
16. A general empirical equation for settling velocities in the Thames was derived:

$$W_n = C^{1.37} \times 1.88 \times 10^{-4} n^{2.34}$$

17. In comparing results from the Thames with those from other estuaries it is observed that the settling index lies consistently between 0.7 and 1.4 showing a universal pattern of behavior. However, absolute values of settling velocity for a given concentration vary by an order of magnitude between estuaries, presumably because k varies with sediment type.
18. No correlation of settling velocity with clay mineral content, particle size or organic content was found between estuaries. This does not rule out the possibility that combinations of these or other parameters may have a significant effect.
19. The Owen tube is still not truly an 'in-situ' measuring device because of the quiescent conditions which exist in it during settling but early indication from current research into deposition from flowing water suggest that it is appropriate because deposition in an estuary only occurs under relatively quiescent conditions.

ACKNOWLEDGEMENTS

This paper is based upon research carried out by Hydraulics Research Limited, Wallingford, United Kingdom, which was partly funded by the UK Departments of Environment and Transport under Research Contract No. DGR/465/36.

Acknowledgements are due to Mr. J. R. Stevenson who organized and carried out the three sets of field measurements and did much of the subsequent analytical work, also to the HR sedimentation laboratory who carried out some 1800 gravimetric suspensed solids determinations.

REFERENCES

1. Allersma, E., Hoekstra, A. J., and Bijker, E. W., "Transport Patterns in the Chao Phya Estuary," Delft Hydraulics Laboratory, Publication No. 47, March 1967.

2. British Standards Institution, "Methods of Testing Soils for Civil Engineering Purposes," BS 1377, 1961.

3. Burt, T. N., and Stevenson, J. R., "Field Settling Velocity of Thames Mud," HR Report No. IT 251, August 1983.

4. Einstein, H. A., and Krone, R. B., "Estuarial Sediment Transport," Proceedings ASCE, Vol. 87, HY2, March 1961, pp. 51-59.

5. Einstein, H. A., and Krone, R. B., "Experiments to Determine Modes of Cohesive Sediment Transport in Salt Water," Journal of Geophysical Research, Vol. 67, No. 4, April 1962, pp. 1451-1464.

6. Happel, J., and Brenner, H., Low Reynolds Number Hydrodynamics, Prentice-Hall, 1965.

7. Hydraulics Research, "Woolwich Ferry Terminals, Field Study of the Effect of Turbulence on Silt Floc Settling Velocities," Report No. EX 467, October 1969.

8. Hydraulics Research, "Thames Flood Prevention Investigation; Analysis of Suspended Solids Regime Prior to Barrier Construction," HR Report No. EX 934, June 1980.

9. Krone, R. B., "Flume Studies of the Transport of Sediment in Estuarial Shoaling Processes," University of California, Hyd. Eng. Lab. and Sanit. Eng. Res. Lab., Berkeley, California, June 1962.

10. Lambe, T. W., "The Structure of Inorganic Soil," Proceeding ASCE, Vol. 79, Separate No. 315, October 1953.

11. Leivich, V. G., Physiochemical Hydrodynamics, Prentice-Hall, Chapter 5, 1962.

12. Migniot, C., "A Study of the Physical Properties of various Forms of very Fine Sediments and their Behavior under Hydrodynamic Actions," La Houille Blanche No. 7, 1968.

13. Neiheisel, J., "Significance of Clay Minerals in Shoaling Problems," Corps of Engineers, U.S. Army, Technical Bulletin No. 10, September 1966.

14. Owen, M. W., "A Detailed Study of the Settling Velocities of an Estuary Mud," HR Report No. INT 78, September 1970.

15. Owen, M. W., "The Effect of Turbulence on the Settling Velocities of Silt Flocs," Proc. Iny. Ass. for Hydraulics Research, 14th Conference, Paris, 1971.

16. Owen, M. W., "The Effect of Temperature on the Settling Velocities of an Estuary Mud," HR Report No. INT 106, July 1972.

17. Owen, M. W., "Determination of the Settling Velocities of Cohesive Muds," HR Report No. IT 161, October 1976.

18. Thorn, M. F. C., and Burt, T. N., "The Silt Regime of the Thames Estuary," HR Report No. IT 175, January 1978.

APPENDIX D1

Analytical port model

An analytical model for predicting mud siltation in the entrance to a tidal basin

II.I Consider the periodic excursion of mud-laden water into a tidal basin, assuming no turbulent exchange in the lateral or vertical directions. The incoming water contains a known concentration of suspended mud, part of which settles within the port, the remainder leaving on the falling tide. Assuming the water is sufficiently deep – a point to be considered later – the maximum excursion of mud into the port, x_{MAX}, will be determined by the tidal amplitude, H, the surface area of the basin, A_s, and the cross-sectional area of the entrance channel, A_c, as follows:–

$$x_{MAX} = \frac{HA_s}{A_c} \qquad \text{....(1)}$$

If the tidal velocity can be assumed to vary sinusoidally with time with the amplitude, u_o, a function of the distance, z, above the bed, it can be expressed as

$$u(z,t) = u_o(z)\sin(wt+\phi_i) \qquad \text{....(2)}$$

Therefore, considering an element of unit width aligned with the centre of the inlet channel, the trajectory of a sediment particle with settling velocity, v_s, entering the channel at height, z_i, when the tidal phase is ϕ_i can be determined from (2) as follows:–

Since

$$\frac{dx}{dt} = u(z,t) = u_o(z)\sin(wt+\phi_i)$$

and

$$\frac{dz}{dt} = -v_s \Rightarrow z = z_i - v_s t$$

then

$$\frac{dx}{dz} = \frac{dx}{dt} \cdot \frac{dt}{dz} = -\frac{u_o(z)}{v_s}\sin(wt+\phi_i)$$

therefore

$$\frac{dx}{dz} = -\frac{u_o(z)}{v_s}\sin\left(w\frac{z_i-z}{v_s}+\phi_i\right)$$

Integrating gives

$$x(z) = -\int_{z_i}^{z} \frac{u_o(z)}{v_s}\sin\left(w\frac{z_i-z}{v_s}+\phi_i\right)dz \qquad \text{....(3)}$$

If $u_o(z)$ is constant or a simple function of z, equation (3) can be evaluated analytically, otherwise a numerical solution would be necessary. In order to illustrate the analytic solution, $u_o(z)$ will be assumed to be constant and equal to the amplitude of the mean tidal velocity averaged over the cross-section of the entrance channel, that is:–

$$u_o = \frac{wHA_s}{2A_c} \qquad \text{....(4)}$$

In this case, the equation (3) can be evaluated to give

$$x(z) = \frac{u_o}{w}\left\{\cos(\phi_i) - \cos\left(\phi_i + w\frac{z_i-z}{v_s}\right)\right\} \qquad \text{....(5)}$$

The point at which a particle settles on the bed (z = o) is, from (5)

$$x(o) = \frac{u_o}{w}\left\{\cos(\phi_i) - \cos(\phi_i + \frac{wz_i}{v_s})\right\} \quad ....(a)$$

or equivalently:– ....(6)

$$x(o) = \frac{2u_o}{w}\sin(\phi_i + \frac{wz_i}{2v_s})\sin(\frac{wz_i}{2v_s}) \quad ....(b)$$

II.2 Only positive values of x are of interest, since any mud which enters the tidal basin and then leaves before settling on the bed is unimportant as far as siltation is concerned. (If the water is sufficiently deep, it is possible for a particle to enter the basin, leave, and then re-enter at a lower height before settling on the bed. This case is, however, treated as if the particle only entered at the lower height before settling on the bed since the incoming concentration at all depths at the entrance is specified as one of the boundary conditions.) For mud to enter the port and settle on the bed, the phase, ϕ_i, at which it must enter must satisfy the condition $0 < \phi_i < \pi$ which means, from equation (6), that the height at which it enters must satisfy $0 < z_i < 2\pi v_s/w$. The case where the depth is less than $2\pi v_s/w$ will be considered in detail later.

II.3 By rearranging equation (6) it can be seen that if a point, x, is accessible to particles entering at phase, ϕ_i, then the heights $0 < z_i < 2\pi v_s/w$ at which it must enter are given by:–

$$z_i = \frac{v_s}{w}\left\{\cos^{-1}(\cos(\phi_i) - \frac{wx}{u_o}) - \phi_i\right\} \quad ....(7)$$

and

$$z_i' = \frac{2v_s}{w}\left\{\pi - \phi_i\right\} - z_i$$

II.4 Similarly, if the mud particles enter at height, z_i, to settle at a point, x, then the tidal phases at which they must enter are

$$\phi_i = \sin^{-1}(\frac{wx}{2u_o\sin(wz_i/2v_s)}) - \frac{wz_i}{2v_s} \quad ....(8)$$

and

$$\phi_i = \pi - \sin^{-1}(\frac{wx}{2u_o\sin(wz_i/2v_s)}) - \frac{wz_i}{2v_s}$$

subject to the constraint $0 < \phi_i < \pi$.

II.5 From equation (7) the point x = 0 can be seen to be reached at all phases of the tide $0 < \phi_i < \pi$ from $z_i = 0$ and from $z_i = 2(\pi - \phi_i)v_s/w$ for $0 < \phi_i < \pi$.

II.6 Any point $0 < x < x_{MAX} = 2u_o/w$ is accessible by mud entering at two heights for the same initial phase of the tide and from the lower of these two heights at two phases of the tide (see equation (8)). The point x_{MAX} is only reached by mud entering at $\phi_i = 0$ from $z_i = \pi v_s/w$.

II.7 Before continuing, consider how, for a fixed point, x, where $0 < x < x_{MAX}$, the height at which the mud enters varies with the phase of the tide in order to settle at the point x. When the initial phase is $\phi_i = 0$, the two heights are given by:–

$$z_i = \frac{v_s}{w}\cos^{-1}(1 - \frac{wx}{u_o})$$

$$z_i' = \frac{2\pi v_s}{w} - z_i$$

As ϕ_i increases, z_i decreases reaching a minimum

$$z_{MIN} = \frac{v_s}{w}\left\{\pi - 2\cos^{-1}\left(\frac{wx}{2u_o}\right)\right\}$$

at

$$\phi_{MIN} = \cos^{-1}\left(\frac{wx}{2u_o}\right)$$

and then increases again returning to the initial point

$$z_i(\phi_i = 0) = \frac{v_s}{w}\cos^{-1}\left(1 - \frac{wx}{u_o}\right)$$

when

$$\phi_i = \phi_{MAX} = \cos^{-1}\left(\frac{wx}{u_o} - 1\right)$$

At the same time, as ϕ_i increases from zero to ϕ_{MAX}, z_i' decreases monotonically to coincide with z_i at

$$z_i' = z_i = \frac{v_s}{w}\cos^{-1}\left(1 - \frac{wx}{u_o}\right)$$

when

$$\phi_i = \phi_{MAX}.$$

If $\phi_i > \phi_{MAX}$ the mud will not settle at the point x for any initial height z_i. It should be noted that ϕ_{MIN} and ϕ_{MAX} are functions of the point, x, being considered.

The mud can therefore be considered as settling from two zones:

1 The lower zone $z_{MIN} < z_i < \frac{v_s}{w}\cos^{-1}\left(1 - \frac{wx}{u_o}\right)$

2 The upper zone $\frac{v_s}{w}\cos^{-1}\left(1 - \frac{wx}{u_o}\right) < z_i' < \frac{2\pi v_s}{w}$

Fig 1 as shown in Fig 1.

II.8 Fig 2 In order to calculate the mass of mud settling at a given point, x, in one tidal cycle consider Fig 2. During a small time, Δt, at a given instant in a tidal cycle, the mass per unit width deposited at a point, x, will be $dM/dt\Delta t\Delta x$. This mud entered the harbour at heights z_i and z_i' at earlier times in the tide (ie $t = -z_i/v_s$ and $t = -z_i'/v_s$ respectively) and the mass balance equation can be written as

$$\frac{dM}{dt}\Delta t\Delta x = u_o(\phi_i)c(z_i)\Delta t\Delta z_i + u_o(\phi_i)c(z_i')\Delta t\Delta z_i'$$

Therefore, the total mass deposited in one tidal cycle is:

$$M = \int_{T_1}^{T_2} u_o(\phi_i)c(z_i)\frac{dz_i}{dx}\,dt + \int_{\tau_1}^{\tau_2} u_o(\phi_i)c(z_i')\frac{dz_i'}{dx}\,dt \qquad \text{....(9)}$$

where $T_2 - T_1$ and $\tau_2 - \tau_1$ are the periods during which mud entered the tidal basin in order to settle at x. From equations (6) and (7)

$$\frac{dz_i}{dx} = \frac{v_s}{u_o}\{\sin(\phi_i + \frac{wz_i}{v_s})\}^{-1}$$

$$\left.\frac{dz_i'}{dx}\right| = -\left.\frac{dz_i}{dx}\right|_{z_i'}$$

For any time t

$$\frac{dt}{d\phi_i} = \frac{1}{w}$$

(9) can therefore be rewritten as

$$M(x) = \frac{v_s}{w}\int_{\phi_L}^{\phi_u} \frac{c(z_i)\sin(\phi_i)d\phi_i}{\sin(\phi_i + wz_i/v_s)} - \frac{v_s}{w}\int_{\phi_L'}^{\phi_u'} \frac{c(z_i')\sin(\phi_i)d\phi_i}{\sin(\phi_i + wz_i'/v_s)}$$

Substituting from (7)

$$M(x) = \frac{v_s}{w}\int_{\phi_L}^{\phi_u} \frac{c(z_i)\sin(\phi_i)d\phi_i}{\sin(\cos^{-1}(\cos(\phi_i) - wx/u_o))} + \frac{v_s}{w}\int_{\phi_L'}^{\phi_u'} \frac{c(z_i')\sin(\phi_i)d\phi_i}{\sin(\phi_i + wz_i/v_s)}$$

Substituting from (7)

$$M(x) = \frac{v_s}{w}\int_{\phi_L}^{\phi_u} \frac{c(z_i)\sin(\phi_i)d\phi_i}{\sin(\cos^{-1}(\cos(\phi_i) - wx/u_o))} + \frac{v_s}{w}\int_{\phi_L'}^{\phi_u'} \frac{c(z_i')\sin(\phi_i)d\phi_i}{\sin(\cos^{-1}(\cos(\phi_i) - wx/u_o))}$$

$$M(x) = \frac{v_s}{w}\{\int_{\phi_L}^{\phi_u} \frac{c(z_i)\sin(\phi_i)d\phi_i}{[1-(\cos(\phi_i) - wx/u_o)^2]^{1/2}} + \int_{\phi_L'}^{\phi_u'} \frac{c(z_i')\sin(\phi_i)d\phi_i}{[1-(\cos(\phi_i) - wx/u_o)^2]^{1/2}}\}$$

....(10)

The first integral in (10) represents the contribution from the lower zone and the second integral represents that of the upper zone. The limits of integration, ϕ_L, ϕ_u, ϕ_L', and ϕ_u', cover the period during which mud can enter the tidal basin in order to settle at the point, x, and will be more fully discussed later.

NOTE If the water is sufficiently deep (ie $D \geqslant 2\pi v_s/w$) then $\phi_L = \phi_L' = 0$ and $\phi_u = \phi_u' = \phi_{MAX}$ and the two integrals in (10) can be combined giving

$$M(x) = \frac{v_s}{w}\int_{o}^{\phi_{MAX}} \frac{\sin(\phi_i)[c(z_i)+c(z_i')]\,d\phi_i}{[1-(\cos(\phi_i) - wx/u_o)^2]^{1/2}}$$

II.9 If it is assumed that $c(z_i) = c(z_i') = c$ (a constant), this integral can be evaluated exactly giving

$$M(x) = \frac{2cv_s}{w}[\cos^{-1}(\cos\phi_i - \frac{wx}{u_o})]_o^{\phi_{MAX}}$$

$$M(x) = \frac{2cv_s}{w}\cos^{-1}(\frac{wx}{u_o} - 1) \qquad ....(11)$$

II.10 This result agrees with the intuitive conclusion that if the mud has a constant concentration and settling velocity, the mass of mud deposited in one tidal cycle will be equal to the settling velocity multiplied by concentration multiplied by the time for which the point, x, is covered by muddy water, ie

$$M = v_s c \Delta t \qquad ....(12)$$

II.11 In this case, the length of time the point, x, will be covered by the incoming tide is

$$\Delta t = \frac{2\pi}{w} - \frac{2}{w}\cos^{-1}(1 - \frac{wx}{u_o}) \text{ since } x = \frac{u_o}{w}(1-\cos(wt))$$

$$= \frac{2}{w}\cos^{-1}(\frac{wx}{u_o} - 1)$$

Therefore, from (12)

$$M(x) = \frac{2v_s c}{w}\cos^{-1}(\frac{wx}{u_o} - 1)$$

which agrees with (11).

II.12 In order to calculate the deposition of mud on the bed the total depth of mud carrying water must be considered. There are three separate cases.

(a) $D \geqslant 2\pi v_s/w$

In this case all the mud entering the port between $z_i = 0$ and $z_i = 2\pi v_s/w$ will, depending on the phase of the tide at which it enters, contribute to the accretion of mud at some point $0 \leqslant x \leqslant x_{MAX}$. The mass deposited at any point, x, is found from equation (10) where the limits of integration are

$$\phi_L = \phi_L' = 0$$

$$\phi_u = \phi_u' = \phi_{MAX} = \cos^{-1}(\frac{wx}{u_o} - 1)$$

(b) $v_s/w \cos^{-1}(1-wx/u_o) < D < 2\pi v_s/w$

In this case for a given point, $0 \leqslant x \leqslant x_{MAX}$, the mud from the lower zone settles as before for tidal phases $0 \leqslant \phi_i \leqslant \phi_{MAX}$. The upper zone, however, has been decreased by the reduced depth and in order for mud to settle at a point, x, the minimum phase of the tide at which it can enter is given by (8):

$$\phi_{MIN} = \pi - \sin^{-1}(\frac{wx}{2u_o\sin(wD/2v_s)}) - \frac{wD}{2v_s}$$

As ϕ increases from ϕ_{MIN} to ϕ_{MAX} so, for mud to settle at x, the height at which it enters decreases from $z_i = D$ to $z_i = v_s/w \cos^{-1}(1 - wx/u_o)$.

(c) $0 < D \leqslant v_s/w \cos^{-1}(1-wx/u_o)$

In this case, the upper flow is absent altogether and the lower flow is reduced. The maximum distance the mud can penetrate is reduced to

$$x_{MAX} = \frac{2u_o}{w}\sin(\frac{wD}{2v_s})$$

The minimum phase at which mud can enter and settle at x is

$$\phi_{MIN} = \sin^{-1}(\frac{wx}{2u_o\sin(wD/2v_s)}) - \frac{wD}{2v_s}$$

and the maximum phase is

$$\phi_{MAX} = \pi - \sin^{-1}(\frac{wx}{2u_o\sin(wD/2v_s)}) - \frac{wD}{2v_s}$$

II.13 The integrals in equation (10) can now be evaluated numerically where the limits, ϕ_L, ϕ_u, ϕ_L' and ϕ_u', are determined according to the depth for a given point, x, as described above.

II.14 Assuming c(z) is non-singular, there is a singularity in the integral when

$$\cos(\phi_i) - \frac{wx}{u_o} = -1$$

However, this singularity is integrable and assuming that c(z) is constant, c, the integrals in (10) can be evaluated giving the following expression for the mass falling at a given point in one tidal cycle:

$$M(x) = \frac{v_s c}{w}\{\cos^{-1}(\cos(\phi_u) - \frac{wx}{u_o}) - \cos^{-1}(\cos(\phi_L) - \frac{wx}{u_o})$$

$$+ \cos^{-1}(\cos(\phi_u') - \frac{wx}{u_o}) - \cos^{-1}(\cos(\phi_L') - \frac{wx}{u_o})\} \qquad ....(13)$$

where

a) if $D > \frac{2\pi v_s}{w}$: $\phi_L = \phi_L' = 0$; $\phi_u = \phi_u' = \phi_{MAX} = \cos^{-1}(\frac{wx}{u_o} - 1)$

b) if $\frac{v_s}{w}\cos^{-1}(1 - \frac{wx}{u_o}) < D < \frac{2\pi v_s}{w}$:

$$\phi_L = 0 \;;\; \phi_L' = \pi - \sin^{-1}(\frac{wx}{2u_o \sin(wD/2v_s)}) - \frac{wD}{2v_s} \;;\; \phi_u = \phi_u' = \phi_{MAX}$$

c) if $0 < D < \frac{v_s}{w}\cos^{-1}(1 - \frac{wx}{u_o})$:

$$\phi_L' = \phi_u' = 0 \;;\; \phi_L = \sin^{-1}(\frac{wx}{2u_o \sin(wD/2v_s)}) - \frac{wD}{2v_s}$$

$$\phi_u = \pi - \sin^{-1}(\frac{wx}{2u_o \sin(wD/2v_s)}) - \frac{wD}{2v_s}$$

If c(z) is a known function of z, the integrals in (10) must be evaluated numerically between the depth dependent limits described above. In this case, the numerical evaluation of the integral must in some cases allow for a singularity at one end of the interval of integration.

II.15 In certain cases it may be possible to represent the flow by two or more layers with different constant concentrations in each layer. In these cases the analytic solution (equation (13)) can be applied to each layer by calculating new limits of integration for each layer. Care would be necessary to ensure that in the calculation of the effect of the upper layers, z_{MIN} does not fall into the layer below. This can be done by splitting the range of integration and carefully calculating the new limits of integration.

II.16 If u_o is a function of z, the trajectory of a sediment particle becomes more complicated. For example, if a logarithmic-type velocity profile is assumed, then as the sediment particle falls towards the bed, its convective velocity decreases both on the ebb and flood tides. Consequently, for low settling velocities, it is possible for a particle to enter the port at a height greater than $2\pi v_s/w$ and still settle on the bed without leaving the channel. These more complicated trajectories require a numerical evaluation of equations (3) onwards but the resulting analysis is still possible and follows the same lines as the analytical method described in this report.

II.17 Since the mass distribution settling on the bed is linearly dependent on the concentration and the settling velocity, and if the mud in suspension consists of different fractions of varying settling velocity and concentration, the total mass distribution on the bed can be found by adding the contributions of the different fractions.

Conclusions

II.18 The analytical model should give a simple and inexpensive solution to the problem of siltation within a tidal basin. The major features of any accretion of mud, for example, the maximum height and length of a mud bar and total masses of deposited mud, should be predictable from a knowledge of the geometry of the basin, the tidal characteristics and the suspended mud. The accuracy of the predictions will depend on the suitability of the assumptions made in deriving the model for the particular situation being considered.

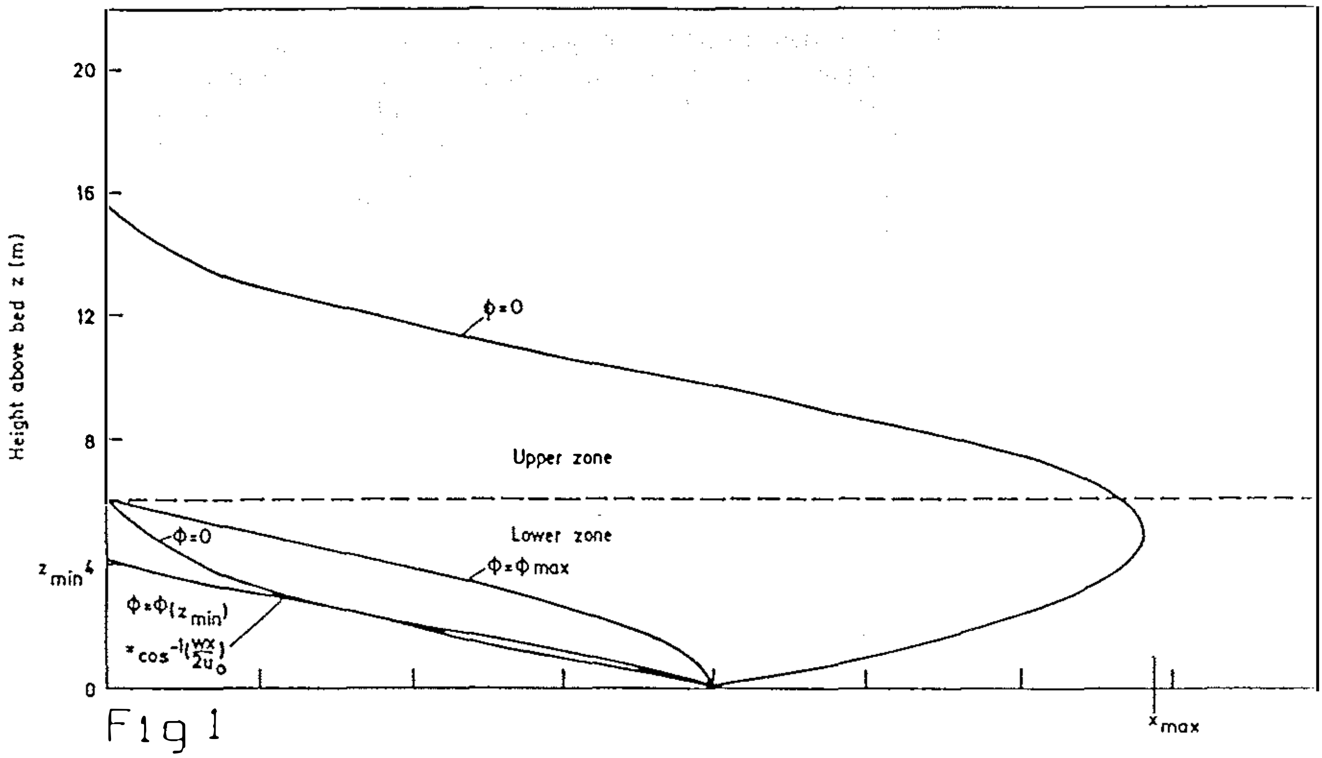

Fig 1

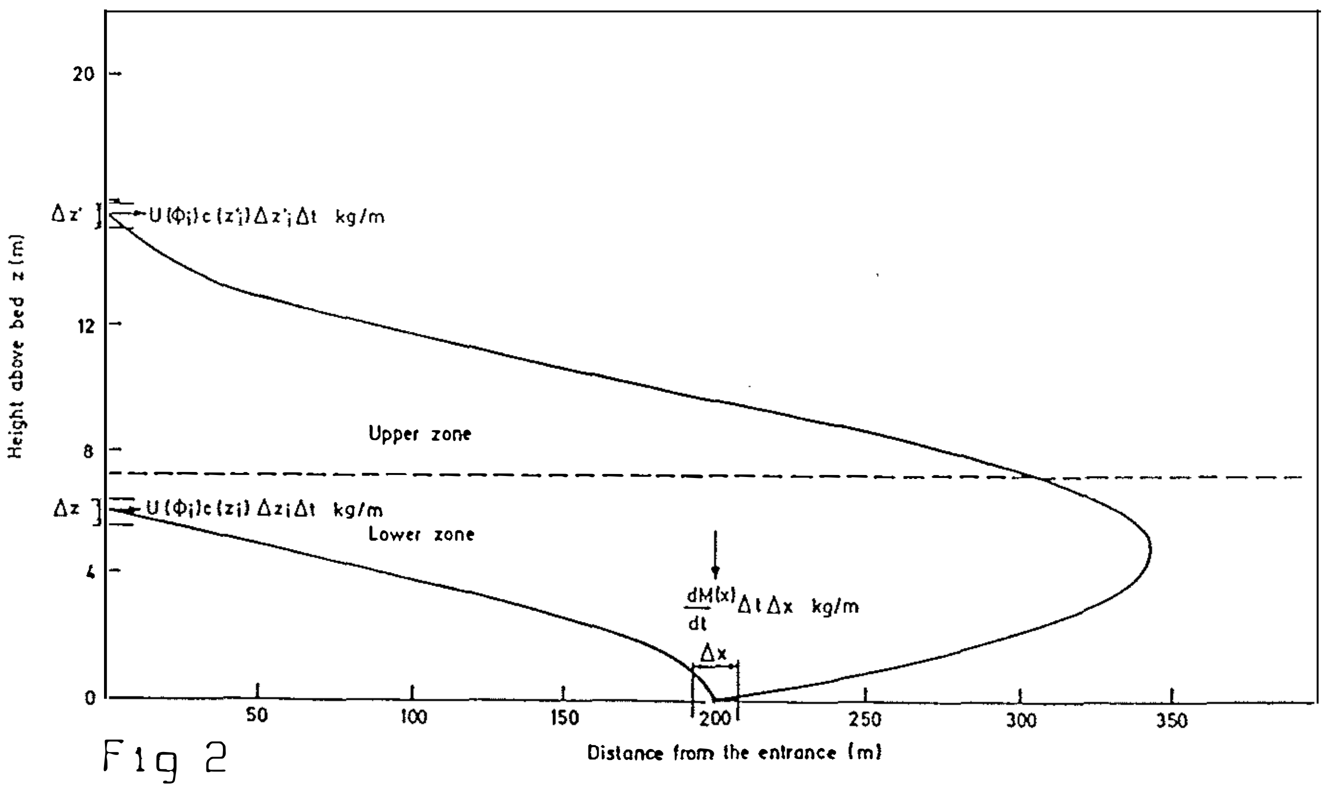

Fig 2

Particle trajectories

APPENDIX E1

Revised plan for field surveys of Tianjin Port disposal area 1988

Attached List

Revised Plan for Field Surveys of Tianjin Port Disposal Area [illegible]

No.	Name	Main Purpose	Area (or Position)	No. of Stations	No. of Surveys	Item	Month	Scale	Legend
1	Sound of Disposal Area	escaping amount of disposed material	3 x 3 sq km		2 times	water depth	beginning & end of the year	1:5000	▭
2	Wave Survey	expanding numerical model programme & varification	-2.5m contour north of the harbour (5km away from Channel)	1	3 months	wave heigh & period	June-Aug		×
3	Survey of Wind Velocity & Direction	wave analysis	gap of North Breakwater	1	3 months	wind velocity & direction	June-Aug		△
4	Hydrologic Data Collection of Disposal Area	current field & silt concentration	5 x 5 sq km	12	synchronization of every 4 stations, per time, 3 times in total (25 hours tidal cycles)	current velocity, direction & silt content	July-Aug		○
				12	circuit of every 4 stations, per time, 3 times in total	silt content			◑
5	Hydrologic Data Collection South & North of the Harbour	expanding numerical model programme & varification	-3 & -6m contour (south of the harbour)	4	2 tidal cycles (spring & neap, one time for each)	velocity, direction, silt content, salinity	ditto		⊗
6	Active Neutron tracer sand	dispersion track & amount of bed soil of disposal area	about 5 x 5 sq km	134	once	sample	ditto		⊙
7	Analysis of magnetizing ratio	trend of soil movement of Tianjin Port	south & north of the harbour	9	once	ditto	ditto		◎ (M)
8	pb 210 analysis	siltation Analysis	ditto	5	once	ditto	ditto		◎ (P)
9	Bed Soil Sample	grain size analysis	ditto	45	once	ditto	ditto		●
10	Survey of Current Path	path of water particle (set up at 0.6 depth)	south & north of disposal area	2	twice	current track	ditto		◎